Dist: A

(1)

AD-A285 262

SC71047.FR

SC71047.FR

Copy No. 2

Processing—Property Relationship in Advanced Intermetallics

Final Report

For Period March 4, 1991 through March 3, 1994

AEOSR-TR- 94 0567

CONTRACT NO. F49620-91-C-0027

Prepared for:

Captain Charles Ward
Air Force Office of Scientific Research/NI
Directorate of Electronic and Material Sciences
110 Duncan Avenue, Suite B115
Bolling AFB, DC 20332-0001

Prepared by:

D. Hardwick
Rockwell Science Center
Thousand Oaks, CA 91360

DTIC
ELECTE
SEP 23 1994
S B D

July 1994

DISTRIBUTION STATEMENT A
Approved for public release;
Distribution Unlimited

94 9 20 046

Rockwell International
Science Center

94-31012

Dist: A

REPORT DOCUMENTATION PAGE

Form Approved
OMB No. 0704-0188

Public reporting burden for this collection of information is estimated to average 1 hour per response, including the time for reviewing instructions, searching existing data sources, gathering and maintaining the data needed, and completing and reviewing the collection of information. Send comments regarding this burden estimate of any other aspect of this collection of information, including suggestions for reducing this burden, to Washington Headquarters Services, Directorate for information Operations and Reports, 1215 Jefferson Davis Highway, Suite 1204, Arlington, VA. 22202-4302, and to the Office of Management and Budget, Paperwork Reduction Project (0704-0188), Washington, DC 20503

1. AGENCY USE ONLY *(Leave Blank)*	2. REPORT DATE	3. REPORT TYPE AND DATES COVERED
	July 1994	Final 03-04-91 through 03-03-94

4. TITLE AND SUBTITLE

Processing—Property Relationship in Advanced Intermetallics (U)

5. FUNDING NUMBERS

F49620-91-C-0027

4. AUTHOR(S)

D.A. Hardwick and P.L. Martin

7. PERFORMING ORGANIZATION NAME(S) AND ADDRESS(ES)

Science Center
Rockwell International Corporation
P.O. Box 1085
Thousand Oaks, CA 91358

7. PERFORMING ORGANIZATION REPORT NUMBER

SC71047.FR
Final Report
AFOSR-TR- 94 0567

9. SPONSORING / MONITORING AGENCY NAME(S) AND ADDRESS(ES)

AFOSR/NI
110 Duncan Avenue, Suite B115
Bolling AFB, DC 20332-0001

9. SPONSORING / MONITORING AGENCY REPORT NUMBER

11. SUPPLEMENTARY NOTES

12a. DISTRIBUTING/AVAILABILITY STATEMENT

Approved for public release,
distribution unlimited

A

12b. DISTRIBUTION CODE

13. ABSTRACT *(Maximum 200 Words)*

The feasibility of using the exothermic reaction between Mo and Si for the synthesis of $MoSi_2$ has been demonstrated. The reaction-HIP process begins with high purity elemental powder and produces a low-oxygen, fully-dense $MoSi_2$ with a grain size of ≈ 40μm. All of the powder handling steps were done in a low-oxygen, inert gas environment to explore the limits of the precautions that are necessary to eliminate SiO_2 contamination. Compression testing of reactively HIP processed material showed that this material enjoys a strength advantage over material processed by HIP from commercial powder. The compression testing was done as a function of temperature, in the range 1200–1450°C, and of strain rate, in the range 10^{-3}-10^{-5}sec^{-1}. The deformation mechanism was determined to be a combination of microcracking and dislocation glide+climb. Large strain deformation resulted in dynamic recrystallization of the $MoSi_2$. Backscatter SEM and TEM were used to characterize the deformed microstructures.

DTIC QUALITY INSPECTED 3

14. SUBJECT TERMS

15. NUMBER OF PAGES
67

16. PRICE CODE

17. SECURITY CLASSIFICATION OF REPORT	18. SECURITY CLASSIFICATION OF THIS PAGE	19. SECURITY CLASSIFICATION OF ABSTRACT	20. LIMITATION OF ABSTRACT
Unclassified	Unclassified	Unclassified	

Table of Contents

Page

Foreword vi

Objective 1

Summary 1

Introduction 2

Experimental Methods and Results 2

Processing Development 2

Mechanical Properties 9

Conclusions 22

References 24

Publications and Presentations 26

Appendix I

D.A. Hardwick, P.L. Martin, S.N. Patankar and J.J. Lewandowski, "Processing-microstructure-property relationships in polycrystalline $MoSi_2$", *Proceedings, International Symposium on Structural Intermetallics,* (1993) pp. 665–674 27

Appendix II

D.A. Hardwick, "Composites Based on Molybdenum Disilicide: Progress and Prospects", to be published in *Intermetallic Composites III,* MRS Spring '94 37

Appendix III

D.A. Hardwick, P.L. Martin and R.J. Moores, "Reaction synthesis of $MoSi_2$ from high purity elemental powders", Scripta Metall. et Mater., 27, (1992) 391-394 50

Table of Contents (Cont'd)

Page

Appendix IV

D.A. Hardwick and P.L. Martin, "Microcracking, Strain Rate and Large Strain Deformation Effects in Molybdenum Disilicide", MRS *Proceedings: Silicides and Refractory Metals,* Fall '93 55

Accession For
NTIS GRA&I ☑
DTIC TAB ☐
Unannounced ☐
Justification
By
Distribution/
Availability Codes
Dist | Avail and/or Special
A-1

List of Figures

Figure		Page
1	Schematic of the processing sequence for $MoSi_2$ from elemental powders	3
2	Time-temperature profile for the HIP schedule	4
3	The microstructure of the powder mixture after 24 hours of ball milling	5
4	Microstructure of (a) air-handled material (3500wppm oxygen) compared with (b) inertly processed material (1600wppm oxygen)	7
5	DTA plot obtained from a sample of CIP powder mixture, Mo+2Si. The solid line represents heatup and the dotted line cooldown	8
6	(a) Microstructure prior to testing and (b) following 6.6% strain in compression at 1400°C/10^{-5} sec^{-1}	11
7	Microstructure in polarized light of specimens deformed (a) 8.7% at 1250°C and (b) 15.2% at 1300°C. Both specimens were compressed at an initial rate of 10^{-4} sec^{-1}	12
8	Microstructure revealed by backscatter SEM contrast of the samples shown in Fig. 7	13
9	Dislocation substructure developed after straining at (a)1300°C and (b) 1400°C	14
10	Compressive stress at 0.2% strain as a function of temperature and strain rate	15
11	In (Flow Stress) vs Reciprocal Temperature	16
12	Flow stress vs strain rate (log-log plot)	18
13	Flow Stress vs Temperature-Corrected Strain Rate (Z)	19
14	The strain rate dependence of the flow stress plotted in the manner of creep data	20
15	Microstructure of $MoSi_2$ strained to 57.3% at 1300°C/$10^{-4}s^{-1}$ as revealed by (a) polarized light and (b) backscatter contrast in the SEM	21
16	Comparison of the flow stress values for $MoSi_2$ with various silica contents	23

Foreword

This Final Technical Report covers the work performed under Air Force Contract F49620-91C-0027 from 3 March 91 through 4 April 94. The contract monitor is Dr. Charles H. Ward of the Air Force Office of Scientific Research.

The program was conducted at the Science Center, Rockwell International Corporation, Thousand Oaks, California. Dr. Dallis A. Hardwick was the program manager and co-principal investigator with Dr. Patrick L. Martin.

Objective

The objective of this research was to use innovative processing to develop controlled microstructures that would result in improved properties in advanced monolithic and composite intermetallic alloys based on $MoSi_2$. These results would be the benchmark for ongoing and future development efforts based on $MoSi_2$.

Summary

This research program integrates a processing-microstructure study on $MoSi_2$ with a microstructure-property evaluation of this same material. This approach allows the greatest possible understanding of the mechanisms linking these three interconnected variables. In the initial phase of the program, processing parameters were determined for the synthesis of high-purity, fully-dense $MoSi_2$. The microstructure and oxygen content of the material at each processing stage were used to gauge the success of the processing strategy and to guide process improvements. As a first step, elemental powders of the Mo and Si were intimately mixed using mechanical alloying. This step did not result in the formation of $MoSi_2$ but did yield the short diffusion distances necessary to ensure $MoSi_2$ formation during subsequent consolidation. Consolidation of the intimately mixed powder produced by mechanical alloying was by cold isostatic pressing (CIP) followed by hot isostatic pressing (HIP). Iterations on the initial HIP and parameters were guided by the results of microstructural characterization. The optimized material had a uniform $MoSi_2$ grain size and was fully dense.

The interrelationships among temperature, stress and strain rate were investigated. This was accomplished through a series of compression tests at temperatures in the range 1200--1450°C and strain rates in the range of 10^{-3} to 10^{-5} sec^{-1}. Analysis of data from these tests allowed determination of the temperature and strain rate sensitivity of $MoSi_2$. Microstructural evaluation revealed that the deformation mechanism was a combination of dislocation glide+climb and microcracking. The microcracking was believed to be a consequence of the unavailability of five independent slip systems due to the very high critical resolved shear stress needed to activated some slip systems in $MoSi_2$. In low purity materials, the lack of slip systems is accommodated by grain boundary sliding. TEM revealed that the nature of the dislocations observed in $MoSi_2$ undergoes a change as the deformation temperature increases from 1300°C to 1400°C. Long straight dislocation segments give way to dislocation loops and tangles. This change could be associated with the BDTT, as it *has* occurred in this temperature range. Under the influence of sufficient strain, $MoSi_2$ dynamically recrystallizes. The temperature/strain rate window for dynamic recrystallization was quite narrow. Higher strain rates and/or lower temperatures will increase the proportion of microcracking, while the combination of lower strain rates and/or higher

temperatures leads to grain growth. Comparison between low and high purity $MoSi_2$ produced by various methods revealed the benefits, in terms of elevated temperature strength, associated with a low silica content.

Introduction

Molybdenum disilicide ($MoSi_2$) is an intermetallic compound that combines a high melting point (2020°C) with excellent resistance to high temperature oxidation [1,2]. These attributes make it a candidate structural material for use at temperatures in the range of 1200° to 1600°C. At ambient and moderate temperatures $MoSi_2$ is brittle; but once the ductile-to-brittle transition temperature (DBTT) is exceeded, it rapidly loses strength. The ductile-to-brittle transition temperature (DBTT) of $MoSi_2$ has been reported to be as low as 950°C [3] and as high as between 1300° and 1400°C [4]. The influence of glassy silica on the DBTT is also under discussion, with claims that it has no influence on the DBTT [4] and counterclaims that the DBTT is decreased in the presence of SiO_2 [5].

Under the auspices of this program, two critical reviews of the literature related to processing-microstructure-property interactions in both monolithic and composite $MoSi_2$ were recently undertaken [6,7]. These reviews are included in this report as Appendices I and II. Together, they provide an up-to-date overview of the current state of research in $MoSi_2$.

Experimental Methods and Results

The following section gives a detailed overview of the experimental methods and the results obtained on this program. It is divided into two subsections: Process Development and Mechanical Properties. Microstructural characterization is included, where appropriate.

Process Development

Our goal in this part of the program was the development of a processing route for high-purity, fully-dense $MoSi_2$. To maximize material purity, the starting materials were elemental powders of Mo and Si. High-purity powders of Mo and Si were obtained from commercial vendors, Table I. The highest priority was placed on obtaining powders with low oxygen contents. Both powders were packed under inert gas by the vendor.

Table I. Characteristics of the Molybdenum and Silicon Powders

Characteristic	*Molybdenum*	*Silicon*
Vendor	ESPI	Noah
Designation	E1670	69198
Mean Particle Size, μm	5	<80
Oxygen Content, wppm	600	20

To maintain material purity, all of the powder handling steps were done in a low-oxygen, inert gas environment. The complete processing sequence is depicted in Fig. 1.

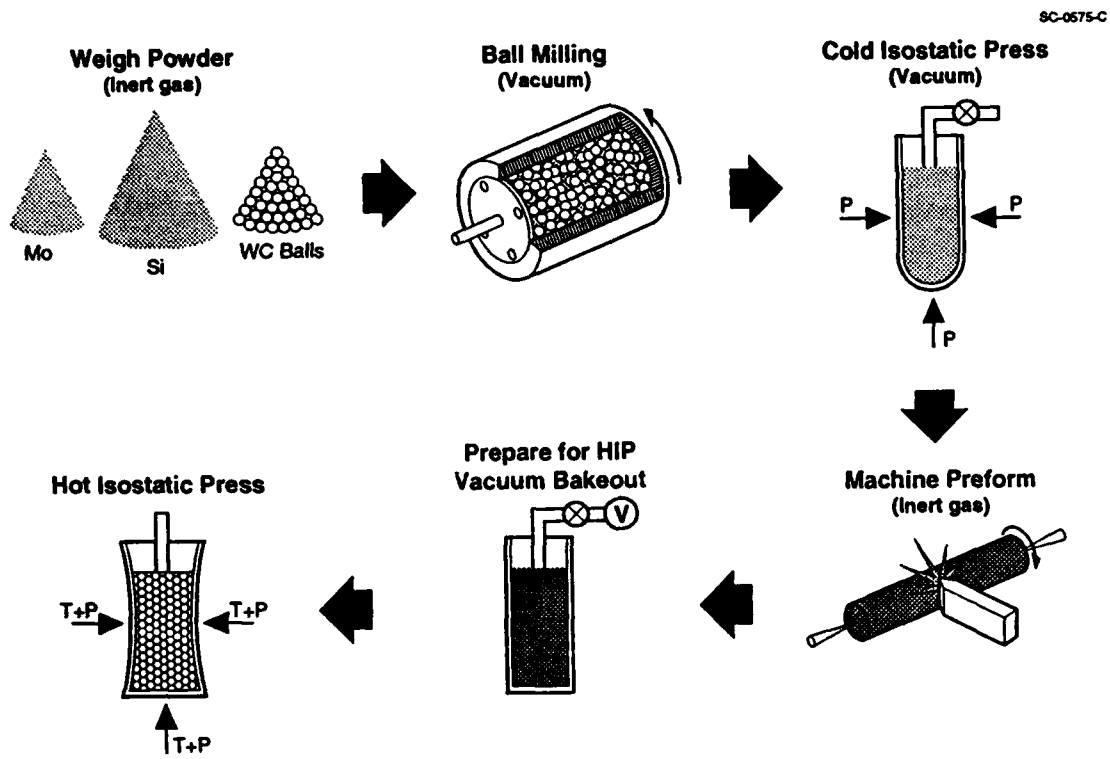

Fig. 1 Schematic of the processing sequence for $MoSi_2$ from elemental powders.

To ensure that the final material produced by the HIP process was as crack-free as possible, the time-temperature schedule shown in Fig. 2 was developed. The slow cooldown from 1400°C was incorporated to minimize cracking that could arise due to the anisotropic CTE of $MoSi_2$. The HIP pressure was allowed to ramp with the temperature and reached 30ksi at 1400°C.

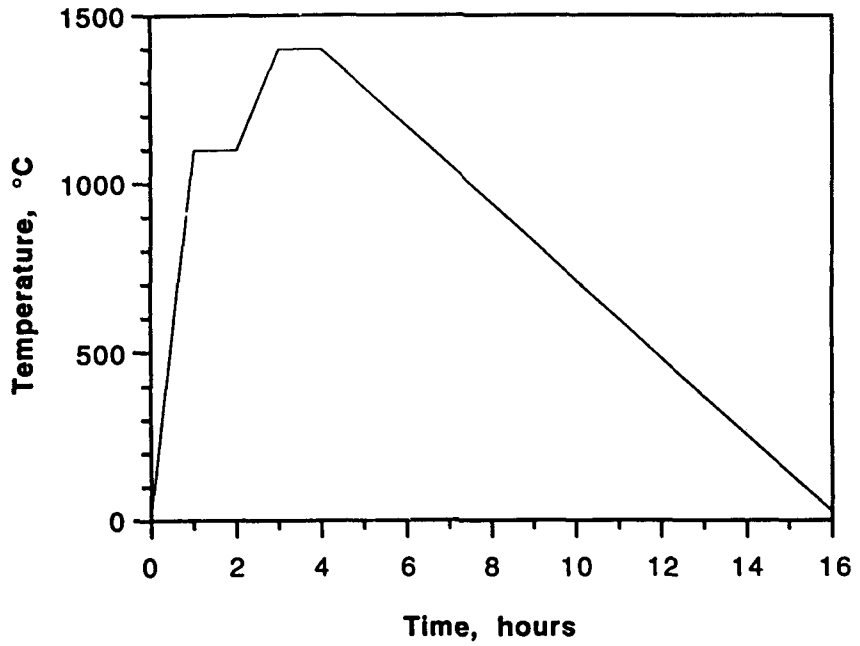

Fig. 2 Time-temperature profile for the HIP schedule.

The following sections give a brief overview of each of the important steps in the processing sequence: ball milling, cold isostatic pressing and hot isostatic pressing.

Ball Milling

To ensure an intimate mixture of the Mo and Si, the elemental powders were ball-milled in an evacuated 300mm diameter stainless steel container using 12mm diameter tungsten carbide balls; the rotation speed was 70 rpm. A powder charge weighing ≈1kg was used, and each charge consisted of the correct amounts of Mo and Si powder to yield stoichiometric $MoSi_2$. The ball:powder weight ratio was 6:1, and no dispersants or additives were used in the milling operation.

During an initial milling run, samples were extracted after time intervals ranging from 1 hour to 150 hours to assess milling efficiency. The powder was mounted and polished and examined both optically and in the SEM. After just 1 hour of milling, there was evidence of deformation in the Mo but little change in the morphology of the Si. Following milling for 8 hours, the Si powder began to fracture into smaller particles, and this process continued through 24 hours of milling time. As shown in Fig. 3, the Mo develops a lamellar structure on ball milling; under the compressive deformation conditions of the ball milling operations, the Mo is quite ductile. The Si on the other hand remains brittle, but fracturing leads to a refinement from the initial Si particle size. After 24 hours, a refined and intimate mixture of the Mo and Si particles was achieved, as shown in Fig. 3.

Fig. 3 The microstructure of the powder mixture after 24 hours of ball milling.

An X-ray spectrum taken from the powder following 150 hours of milling indicated that mechanical mixing and comminution were the only processes that had taken place. There was no evidence of either amorphization or compound formation.

Cold-Isostatic Pressing

Following ball milling, the resultant powder was sieved and then tightly packed into a flexible rubber sleeve (38mm diameter) for cold isostatic pressing (CIP). The impervious rubber container was evacuated to a measured pressure of 4×10^{-3} Pa (3×10^{-5} torr). Cold pressing was accomplished at 200 MPa for 30 minutes. The resultant "green body" had a measured density of 67% and sufficient strength to permit machining to a tight tolerance before placement within cylindrical Ta HIP cans, 25 mm in diameter and 76 mm high.

In our initial experiments, the machining of the CIP compacts was done in air. This led to oxygen contamination of the CIP material, amply demonstrated by the dramatic rise in temperature of the CIP compact when it was removed from the inert atmosphere of the glovebox prior to machining. This was obviously unacceptable. Following acquisition of a small lathe, the machining of the CIP preform for subsequent runs was accomplished in the inert atmosphere of the

glove box. The results of this total inert handling were manifested in both the chemical composition and the microstructure of the $MoSi_2$. Analysis of material from a run machined in air, revealed an oxygen concentration of 3500 wppm while an inertly handled material, machined in argon, contained only 1600 wppm oxygen.

A comparison of the microstructures of these two materials is afforded in Fig. 4. The most significant difference between the two materials lies in their grain size. Despite identical processing conditions, the higher purity material has a larger grain size. Presumably the SiO_2 particles hinder grain growth; the smaller volume fraction of SiO_2 particles in the higher purity material is quite evident.

Hot Isostatic Pressing

During the hot isostatic pressing (HIP) cycle, a strong exothermic reaction occurs as Mo and Si form $MoSi_2$. This is demonstrated in Fig. 5, which shows a DTA scan performed on a ball-milled, cold-pressed powder mixture. At the heating rate of 40°C/min shown in Fig. 5, the exotherm occurred at 1320°C. (The DTA was calibrated using the melting point of Cu.) This onset temperature is well below both the melting temperature of silicon (1414°C) and the Mo-Si eutectic temperature (1400°C), indicating that the reaction initiates in the solid state before Si melting can occur.

This is in strong contrast to the behavior reported for the reaction synthesis of the intermetallic compounds Fe_3Al and FeAl from elemental powders [8]. Heating of powder mixtures of Fe+Al yielded a small exothermic peak at temperatures below the Fe-Al eutectic temperature (625°C), but the predominant peak that marked a strong exothermic reaction was observed near the melting point of aluminum. Compound synthesis was associated with the formation of a transient liquid phase that originated and spread outward from the aluminum particles. However, the Fe (6-9 μm) and Al (10 μm) powders used in this study were merely mechanically mixed prior to cold pressing. In contrast, as shown in Fig. 3, the average size of individual Mo or Si particles is considerably smaller than 10 μm, and the ball milling process has cold-welded agglomerates of these particles into intimate contact. The combined effect of a fine particle size and many cold welded surfaces of Mo and Si appears to facilitate the solid state reaction.

The conditions chosen for the initial HIP runs were: 1 hour to 1400°C, 1 hour hold, 4 hour ramp to RT. The pressure was allowed to increase with the temperature to a maximum of 200MPa. Following this HIP cycle, the powder had completely reacted to form $MoSi_2$, but the product was cracked and quite porous. This cracking and porosity could have arisen from two causes. The primary cause was most likely the relatively fast cooldown rate to ambient temperature. $MoSi_2$ has a noncubic crystal structure, which results in highly directional CTE values. Thus, polycrystalline

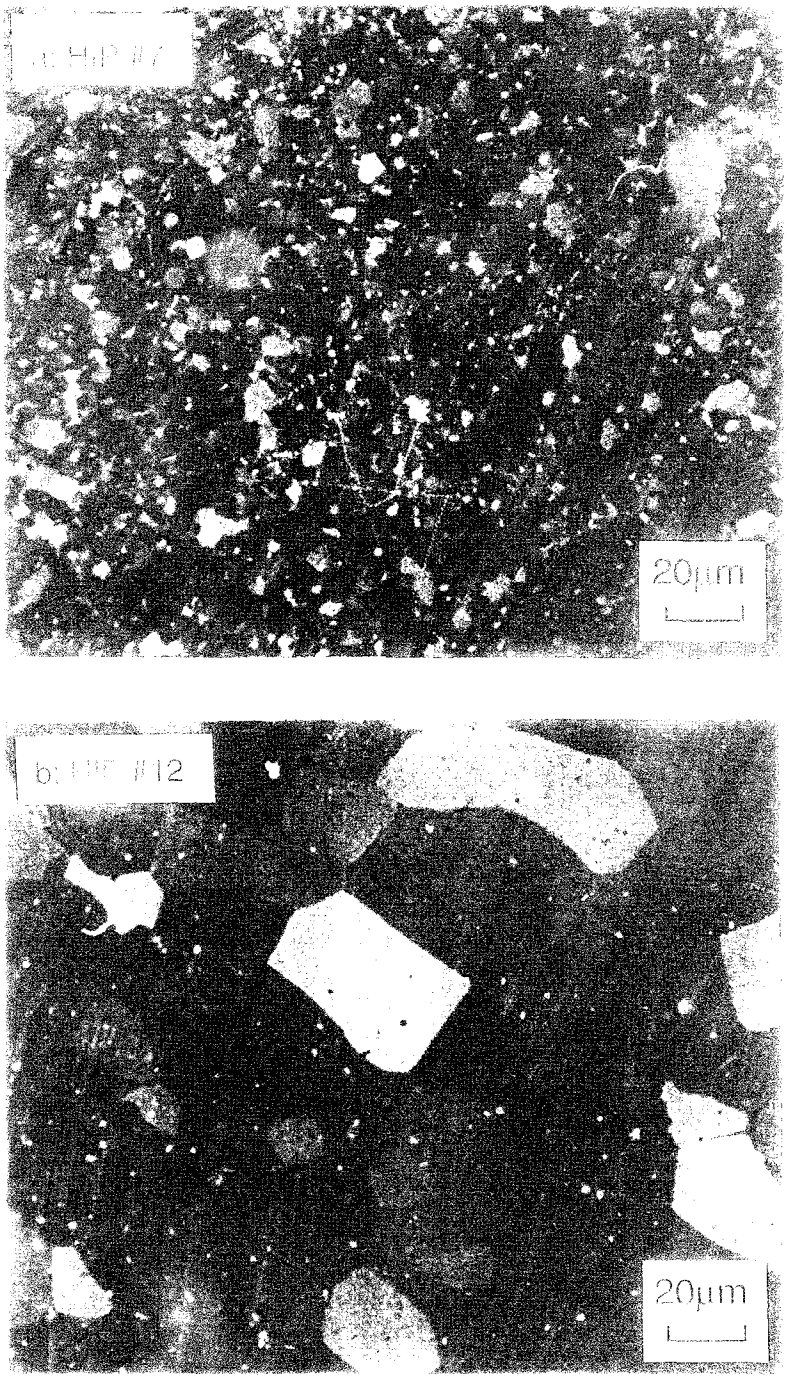

Fig. 4. Microstructure of (a) air handled material (3500wppm oxygen) compared with (b) inertly processed material (1600wppm oxygen).

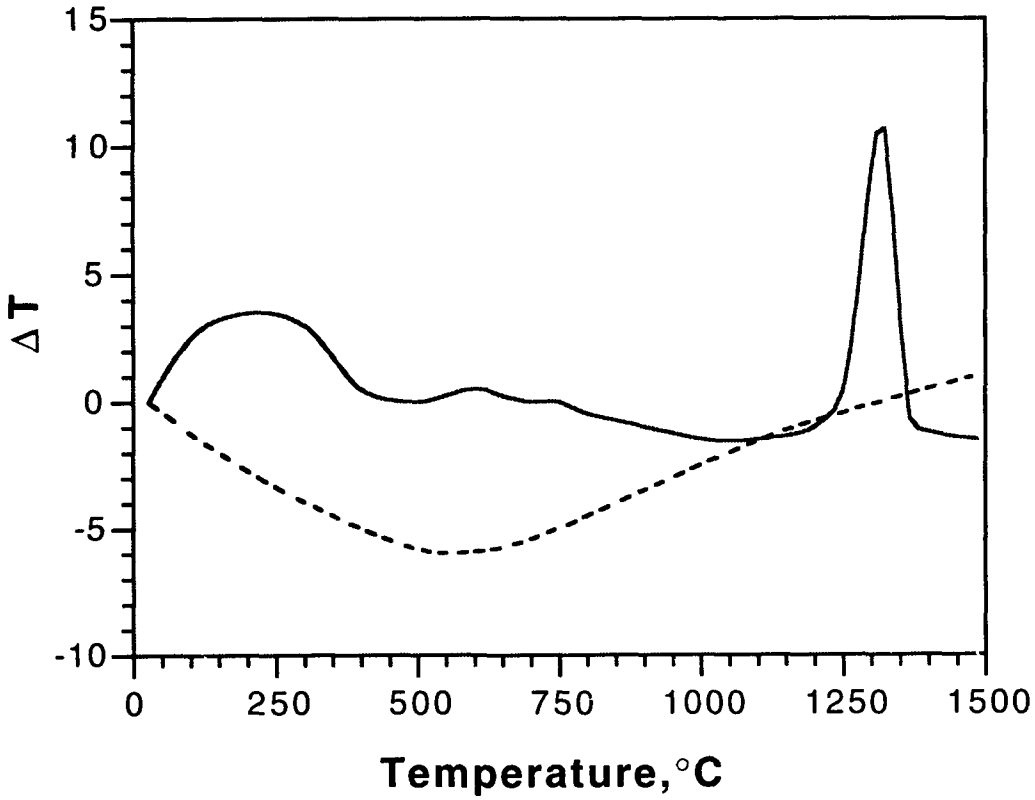

Fig. 5 DTA plot obtained from a sample of CIP powder mixture, Mo+2Si. The solid line represents heatup and the dotted line cooldown.

$MoSi_2$ is quite prone to cracking if cooled at a rate that is too high to permit accommodation of the CTE within the microstructure. To alleviate this source of cracking, the time for cooldown from 1400°C to room temperature was increased from 4 to 12 hours. A further cause of the porosity and cracking was the possibility of nonuniform ignition of the exothermic reaction. The ramp to 1400°C over 1 hour might not provide sufficient time for the entire powder compact to come to a uniform temperature. This would result in nonhomogeneous ignition of the reaction. The porosity was concentrated towards the center of the HIP can; this could arise if ignition of the reaction occurred first at the outer edge of the compact. Consequently, a short hold at 1100°C was programmed into the HIP temperature profile; this hold at 1100°C, well below the reaction temperature, should allow the powder compact to equilibrate to a uniform temperature prior to initiation of the exothermic reaction.

The incorporation of both of these modifications resulted in the following HIP cycle which was used for all subsequent runs: 1 hour to 1100°C, 30 minute hold, 1 hour to 1400°C, 1 hour hold, 12 hour ramp to RT with the pressure rising and falling with the temperature. This HIP cycle was

illustrated schematically in Fig. 2. Material reacted using this HIP cycle was dense and exhibited only minor amounts of cracking around the perimeter of the HIP can.

Mechanical Properties

With the processing schedule fixed, the next goal of this program was the determination of the **intrinsic** mechanical properties of polycrystalline $MoSi_2$ as a function of temperature and strain rate. As a consequence of our process development efforts, two grades of $MoSi_2$ were available for testing. The microstructures of these two materials, designated low purity and high purity in the remainder of this report, were illustrated in Fig. 4. The low purity material resulted from air exposure during machining of a CIP compact that ultimately became HIP#7. This material had a grain size of ≈10 μm and an oxygen content of 3500 wppm. The high purity material was produced from inertly processed powder compacts in 3 HIP runs: #10, #12 and #13. These materials exhibited an average grain size of ≈ 40 μm and oxygen levels ranging from 600 wppm (HIP #13) to 2000 wppm (HIP #10).

Compression Test Procedure:

Right circular cylinders for compression testing were electro-discharge-machined from the HIP compacts; the diameter of an average cylinder was 9.5 mm and the length was 10 mm. The ends of the cylinders were polished flat and perpendicular to the cylinder axis. Compression testing was performed over a range of strain rates from 10^{-3} to $10^{-5}sec^{-1}$. All testing was conducted in a vacuum of 5×10^{-3} Pa or better and at temperatures in the range 1200° to 1450°C. The compression platens were silicon nitride, and the specimens were lubricated with boron nitride to reduce frictional effects. The silicon nitride platens were not deformed by the testing procedure; they did crack following a cycle of several tests and when this occurred, the platens were replaced. After testing, the cylinders were sectioned vertically and the microstructures examined optically and in the SEM.

All of the tests were terminated at strains greater than 1% (all strain values mentioned are plastic), the lowest being 1.4% strain in the specimen tested at 1200°C and a strain rate of 10^{-4} sec^{-1}. The majority of the tests were terminated at strains of 13–15%.

None of the samples from HIP #7 (low purity) or HIP #10 and #12 (high purity) exhibited cracking on the external surfaces. Compression specimens from HIP #13 showed extensive cracking. This was attributed to the material having been shipped twice across the country, to the University of Michigan and back, prior to testing. Some samples from this HIP run cracked so badly on testing that the loading curve declined rapidly from its peak value. The results from such tests were discarded, as we could not determine whether general yielding had occurred prior to sample breakup.

Microstructural Response

Metallographic examination of macroscopically uncracked samples of high purity $MoSi_2$ sectioned longitudinally revealed that all of the samples contained internal microcracks, both transgranular and intergranular. The microcracking was not reflected in the recorded stress-strain curves; these curves exhibited the usual nonlinearity associated with "normal" plasticity. Typically, the transgranular cracks traversed just one or two grains before stopping, as shown in Fig. 6.

Ghosh et al. [9] also observed both transgranular and intergranular cracks in $MoSi_2$ following compression testing. Such microcracking is probably the direct result of the large variation in the critical resolved shear stress (CRSS) for glide of variously oriented $MoSi_2$ grains [10,11]; some orientations will be more amenable to slip than others, leading to stress concentrations at grain boundaries with certain orientations. The observation of very nonuniform dislocation densities in strained $MoSi_2$, with dislocation-free grains adjoining dislocation-rich grains is consistent with this mechanism [12]. In addition, plastic flow itself can initiate cracking in $MoSi_2$; atomically sharp cracks have been observed in the region of severe strain gradient under hardness indentations [13].

In their barreled regions, these specimens also contained intergranular cracks. Intergranular separation could also arise from the juxtaposition of "soft" and "hard" oriented grains as adjacent grains would be unable to deform cooperatively. This effect would be exacerbated by the tensile stresses that will develop in the barreled regions of compression samples.

In contrast, the low purity material did not contain microcracks. In impure, high silica material, microcracking may not occur, as the stress would be dissipated through viscous sliding of the grain boundary silica film before the critical stress to nucleate cracks could be achieved. Metallographic examination revealed that the microstructure of the impure materials was essentially unchanged by the imposition of $\approx$ 15% strain.

Metallographic examination of the high purity samples deformed to plastic strains $\leq$15% with polarized light revealed that the grain boundaries, which were quite straight prior to deformation as shown in Fig. 3, had developed a wavy character. The degree of waviness was greatest in samples that had received the highest amount of strain. Figure 7(a) shows a sample compressed 8.7% at 1250°C while the sample in Fig. 7(b) was strained 15.2% at 1300°C; both were strained at a rate of 10^{-4} sec^{-1}. Both samples exhibit the wavy grain boundary effect but it is most prominent in the more highly strained sample.

Examination of these same samples using backscatter contrast in the SEM reveals further differences. Backscatter imaging delineates the minor orientation differences that arise from subgrains. This contrast is well-developed in the more highly strained sample of Fig. 8 (b) but

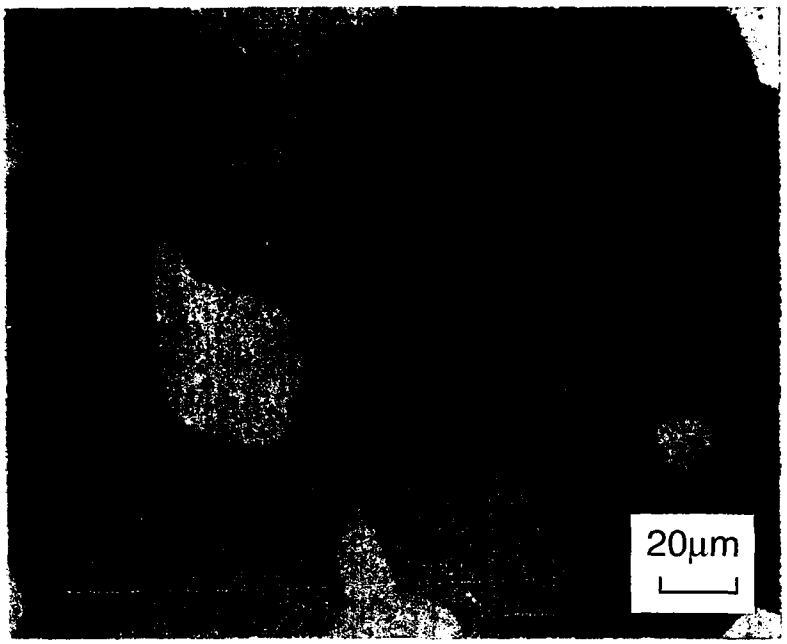

(a)

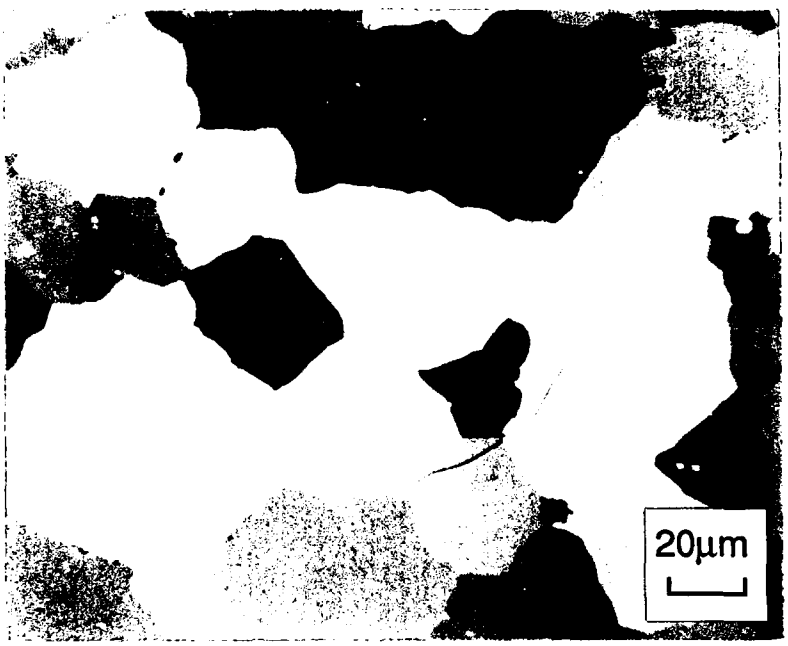

(b)

Fig. 6 (a) Microstructure prior to testing and (b) following 6.6% strain in compression at 1400°C/10^{-5} sec^{-1}.

(a)

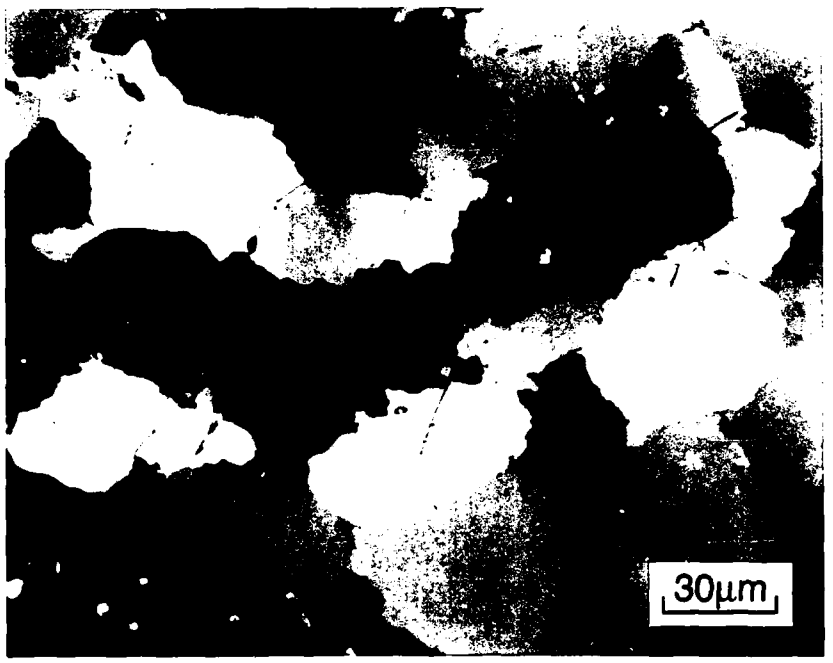

(b)

Fig. 7 Microstructure in polarized light of specimens deformed (a) 8.7% at 1250°C and (b) 15.2% at 1300°C. Both specimens were compressed at an initial rate of 10^{-4} sec^{-1}.

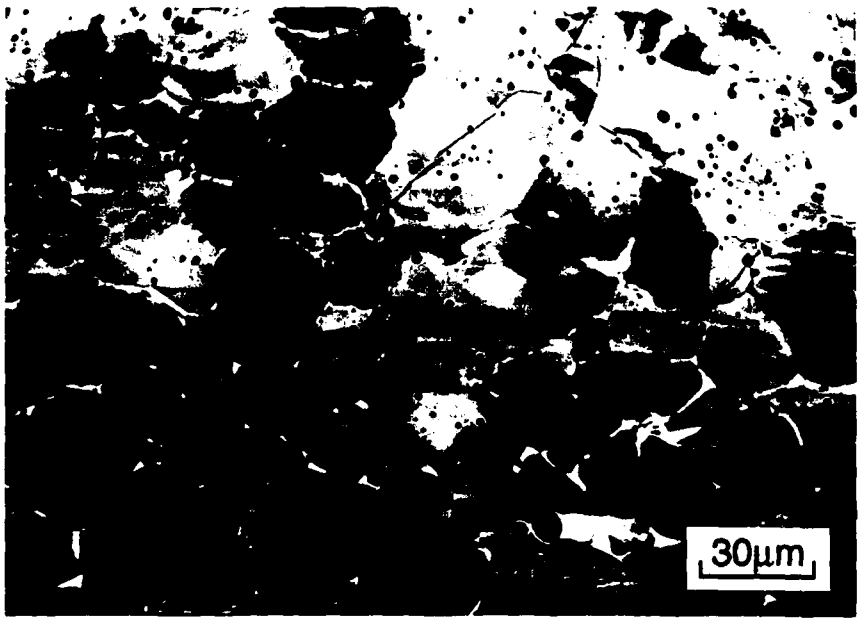

(a)

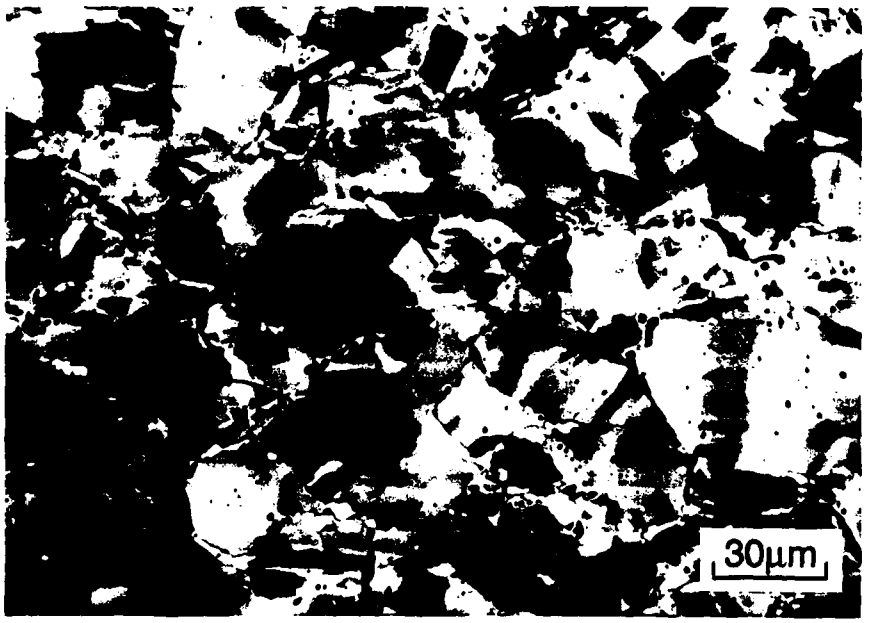

(b)

Fig. 8 Microstructure revealed by backscatter SEM contrast of the samples shown in Fig. 7.

almost absent in Fig. 8 (a). Examination at higher magnification showed that the waviness of the grain boundaries is associated with individual subgrains within the grains.

Regardless of strain rate, deformation at 1400°C resulted in grain growth. Temperature alone was not sufficient to cause grain growth at 1400°C; a sample held at this temperature for 1 hour (a typical time to completion for a straining experiment) did not exhibit grain growth.

TEM examination revealed that straining at 1300°C and 1400°C gave rise to very different dislocation substructures; this is illustrated in Fig. 9. At 1300°C, the dislocation segments are quite straight and tend to form arrays and low angle boundaries within the microstructure. At 1400°C the dislocations are quite wavy and many loops are observed. These may be indicative of thermally activated mechanisms such as dislocation climb. Work is continuing to gain a more quantitative understanding of the differences between these two dislocation substructures. However, we can conclude that there is a significant change in deformation character between 1300°C and 1400°C. This may offer definitive evidence for the intrinsic DBTT of $MoSi_2$ falling between 1300°C and 1400°C.

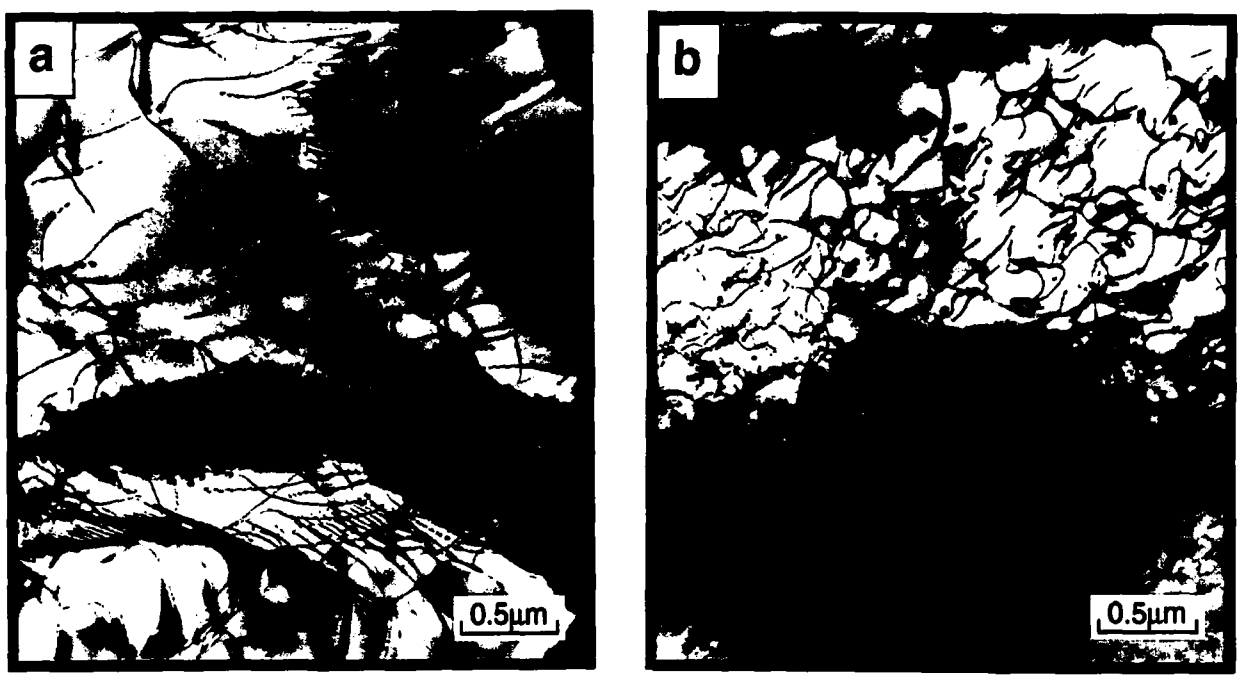

Fig. 9 Dislocation substructure developed after straining at (a) 1300°C and (b) 1400°C.

Effect of Temperature on Flow Stress

The 0.2% offset compressive yield stress as a function of temperature and strain rate is plotted in Fig. 10 for both our low and high purity $MoSi_2$. The lines drawn through the data are curves of best fit using a least squares formalism. The effect of oxygen (silica) contamination is easily seen; the low purity material tested at $10^{-4}s^{-1}$ is significantly weaker than the higher purity material tested at $10^{-5}s^{-1}$.

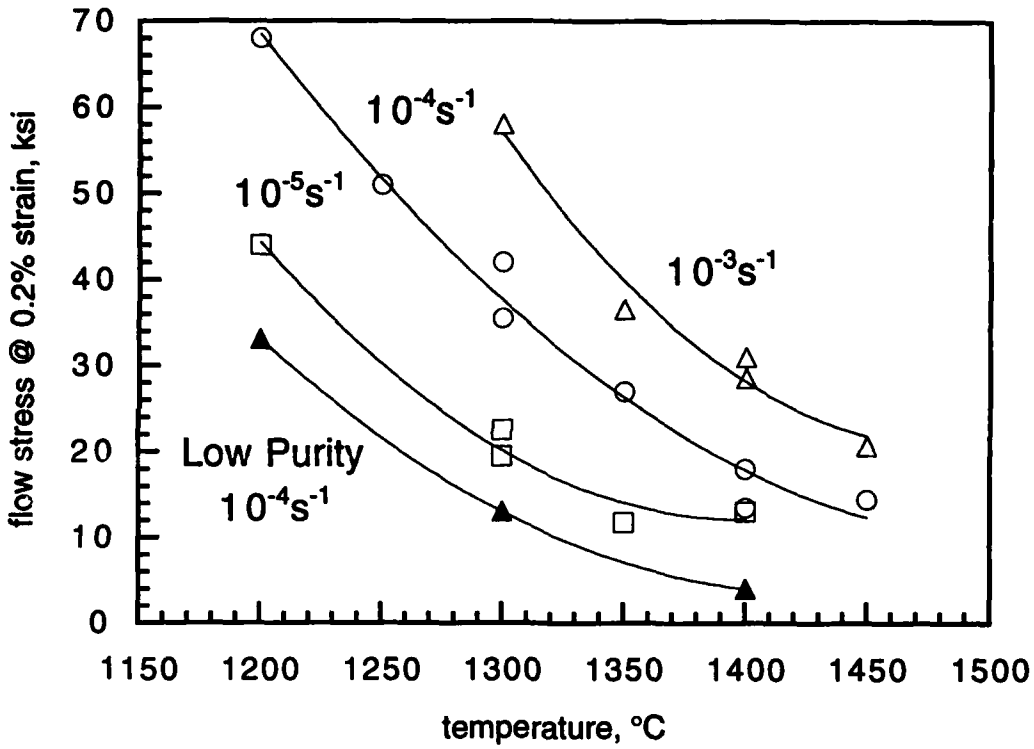

Fig. 10 Compressive stress at 0.2% strain as a function of temperature and strain rate.

As the test temperature increases, the flow stress decreases but the rate of decrease diminishes with increasing temperature. In general, the temperature dependence of the flow stress at a given strain can be expressed as:

$$\sigma = (\text{const}) \exp (Q / RT)$$

The activation energy, Q, associated with the temperature dependence of the flow stress can be determined from a plot of ln σ versus 1/T as shown in Fig. 11. Using the graphics application Kaleidagraph™, the equation of each line is obtained in the form y=a+bx. The calculated values of Q are listed in Table II.

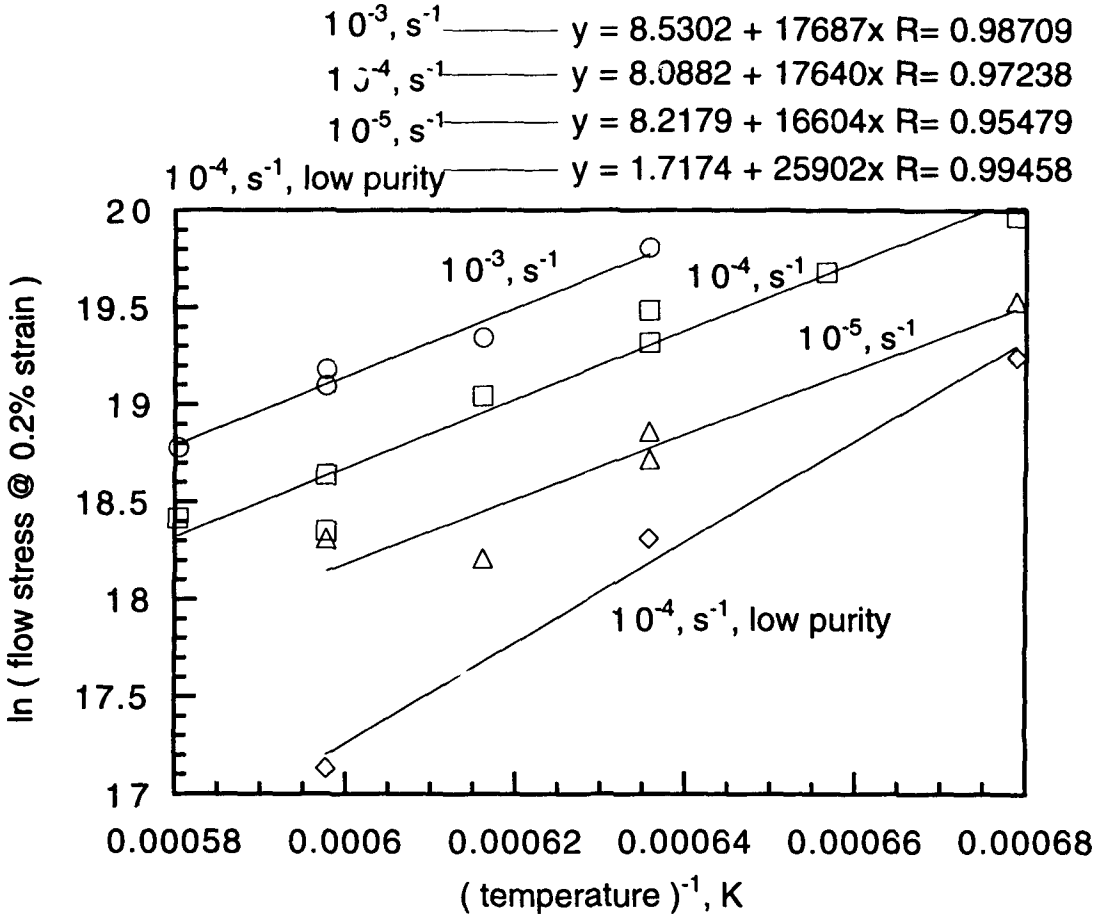

Fig. 11 In (Flow Stress) vs Reciprocal Temperature.

Table II: Calculation of Activation Energy for the Flow Stress

Material:	Strain Rate, s^{-1}	Q, kJ/mol
High Purity $MoSi_2$	10^{-3}	147.0
	10^{-4}	146.7
	10^{-5}	138.1
Low Purity $MoSi_2$	10^{-4}	215.4

This data indicates that the deformation of the lower purity $MoSi_2$ is more strongly influenced by temperature than is the higher purity material.

Effect of Strain Rate

Figure 10 also indicates that the flow stress for the pure material is strain rate sensitive. At a constant temperature and strain, the relationship between the flow stress, σ, and the strain rate, $\dot{\varepsilon}$, is given by:

$$\sigma = \text{const} (\dot{\varepsilon})^m$$

where m is the strain rate sensitivity. The value of m is obtained from a log-log plot of the flow stress versus the strain rate as shown in Fig. 11. Again the graphics application Kaleidagraph™ has been used to obtain the equation of each line, this time in the form: $y=ax^b$ where b is the strain rate sensitivity parameter, m.

Using only the values at the temperatures for which we obtained more than two data points, the average m value is 0.22. This value indicates that the deformation of high purity $MoSi_2$ in this temperature range is only moderately sensitive to strain rate.

Combined Effect of Temperature and Strain Rate

The combined effects of temperature and strain rate on the flow stress of a material can be assessed through Z, the Zener-Holloman parameter which is defined as:

$$Z = \dot{\varepsilon} \exp (\Delta H / RT)$$

where ΔH is the activation energy and is related to Q through m, the strain rate sensitivity parameter: $Q = m (\Delta H)$. ΔH is independent of both temperature and strain rate.

We have already determined for the high purity material that $Q \approx 144$ kJ/mol and $m \approx 0.2$; therefore $\Delta H = 720$ kJ/mol. This value is used to plot the data for the high purity material onto one curve as a function of Z, the temperature corrected strain rate, in Fig. 13. The equation of this curve can then be used to calculate the flow stress for our high purity $MoSi_2$ for any combination of temperature and strain rate, provided it does not fall much beyond the region of our initial data. The reason for this caveat is that as the value of Z increases (i.e., temperature decreases, strain rate increases) the yield stress will reach a limiting (athermal) value [14].

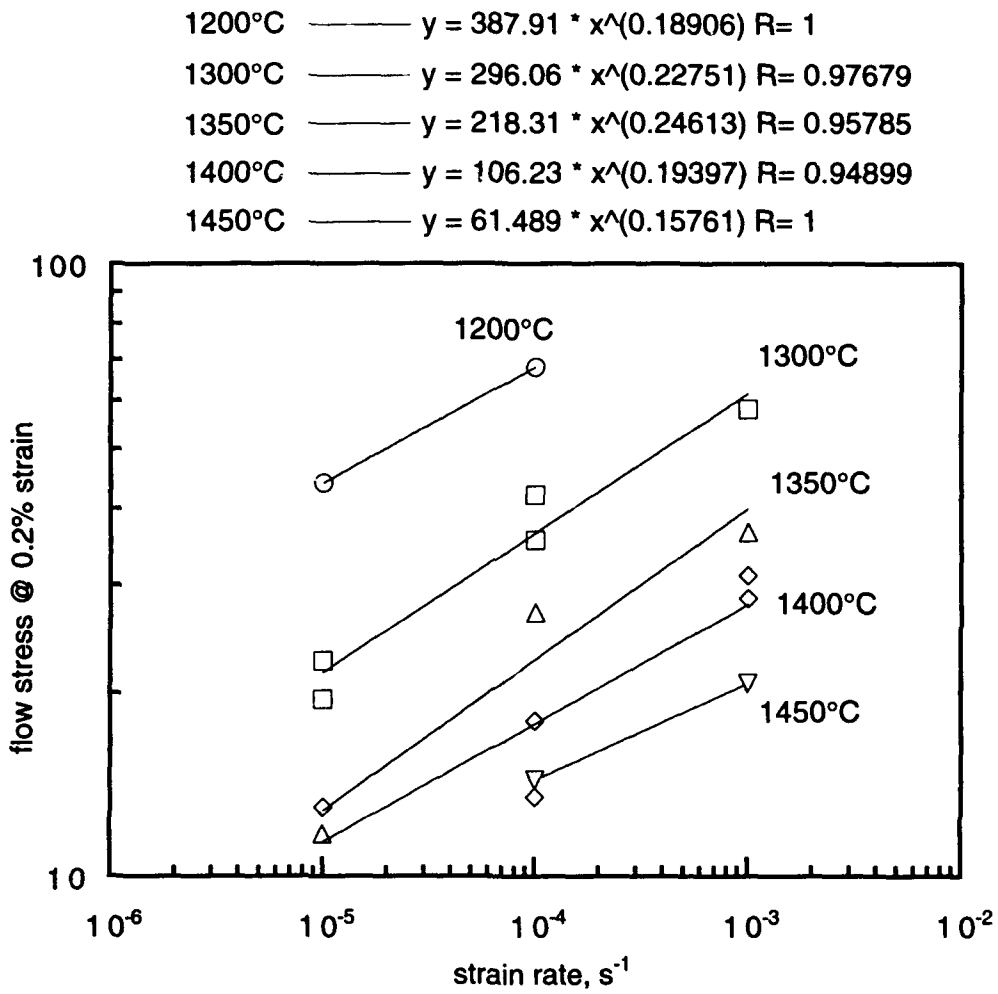

Fig. 12 Flow stress as a function of strain rate (log-log plot).

This analysis is not possible for the impure material as, although we know the sensitivity of this material to temperature (Q ≈ 215 kJ/mol), we have not determined its strain rate sensitivity, m. If ΔH remains constant at 720 kJ/mol, then the m value of the lower purity material will be 0.3. This is not an unreasonable value; we would expect a material with finer grain size to exhibit greater strain rate sensitivity.

Creep Analysis

The strain rate and temperature dependence of the flow stress can also be analyzed in a manner analogous to creep data. The power relation of creep behavior is:

$$\dot{\varepsilon} = (\text{const})\ \sigma^n \exp(-Q/RT)$$

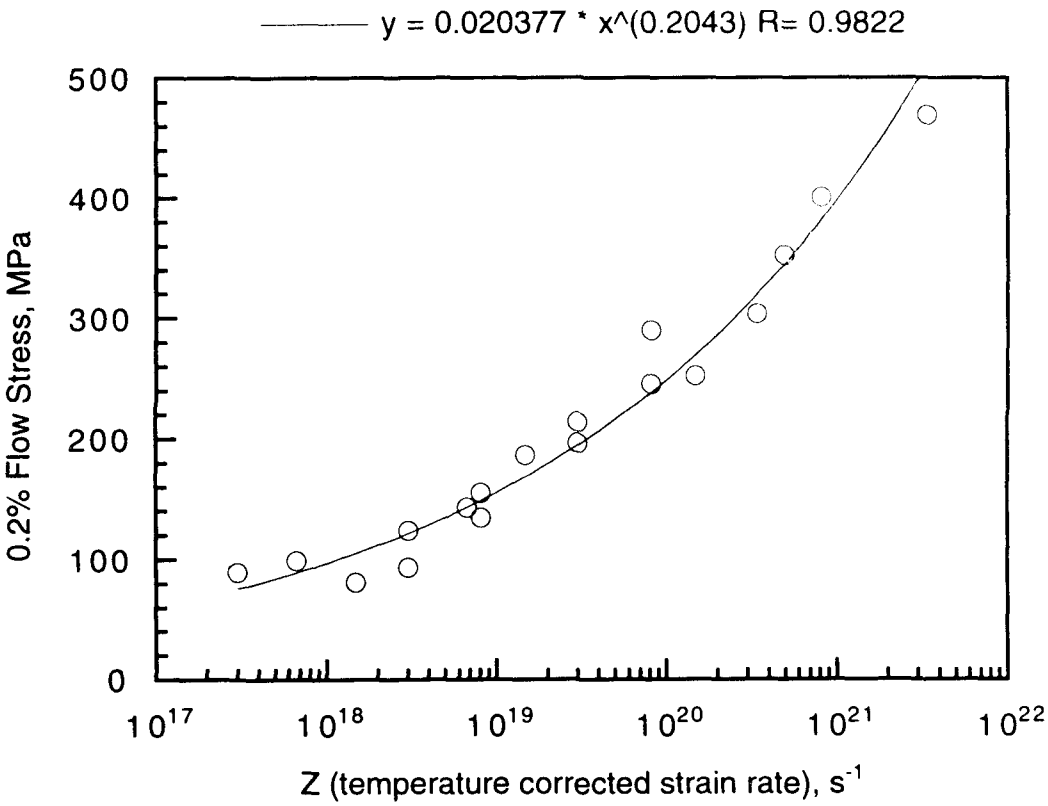

Fig. 13 Flow stress as a function of temperature-corrected strain rate (Z).

From a log-log plot of the strain rate versus the flow stress at given temperature we can determine the stress exponent, n. This analysis is shown in Fig. 14, which plots data at 1300°, 1350°C and 1400°C, the temperatures where we have flow stress data at three strain rates. The stress exponent value falls between 3.8 and 4.3. Bose [15] observed stress exponents of $n \geq 3$ for $MoSi_2$ produced by a variety of methods. Stress exponent values in the range of 3–4 imply that dislocation climb is rate controlling. On the other hand, Sadananda et al. [16] found a stress exponent of 2 for the creep of hot pressed $MoSi_2$ supplied by Los Alamos National Laboratory. Our review [7] has shown that this material has very poor strength, probably due to a high silica content. Therefore, the stress exponent value of 2 most probably reflects deformation by a combination of dislocation climb and grain boundary sliding on viscous silica grain boundary films.

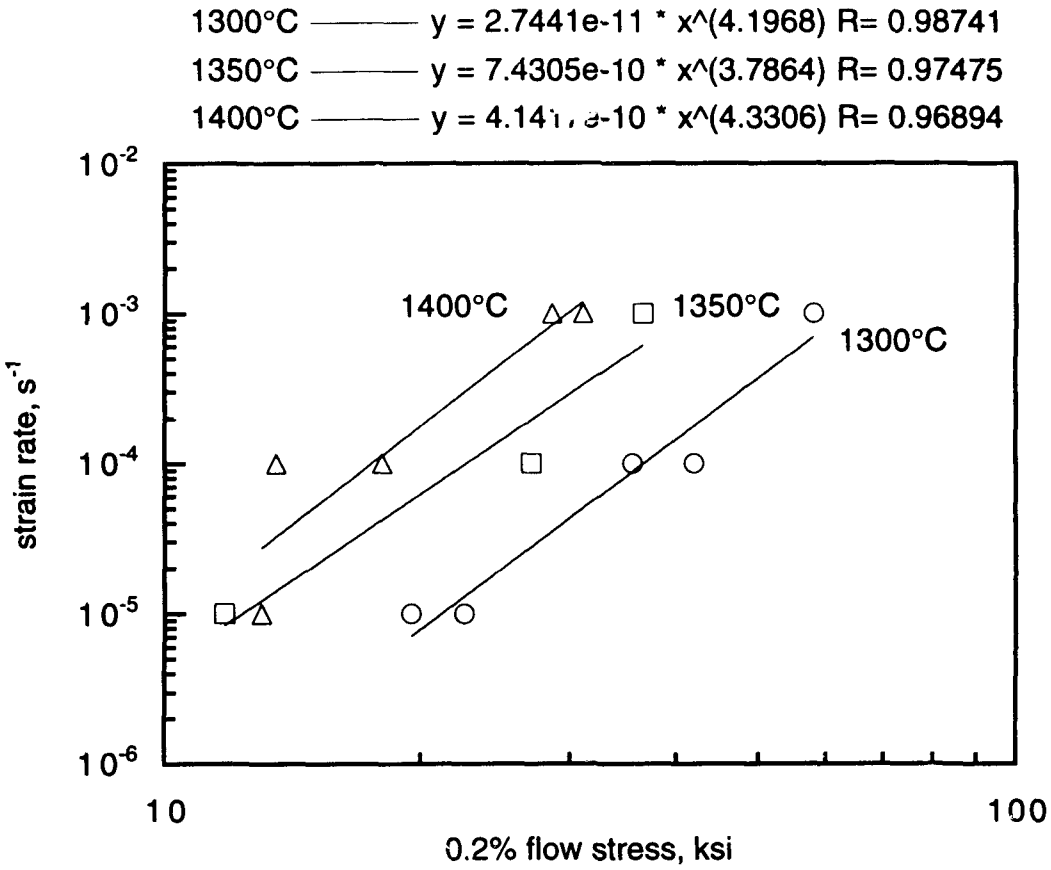

Fig. 14 The strain rate dependence of the flow stress plotted in the manner of creep data.

Large Strain Deformation

The deformation of $MoSi_2$ to very large strains was also investigated. To avoid grain growth, samples were strained at 1300°C at strain rates of 10^{-4} and 10^{-5} sec^{-1}. The microstructure of the sample strained 48.5% at 10^{-5} s^{-1} exhibited only minor distortion of the grain shape in response to the imposed strain and very limited evidence of recrystallization. On the other hand, the microstructure after 57.3% strain at 10^{-4} s^{-1} consisted of pancake shaped grains plus significant regions of recrystallized grains surrounding the larger pancakes. This is shown in the polarized light micrograph in Fig. 15(a). The backscatter contrast micrograph in Fig. 15(b) reveals the extent of subgrain formation within the deformed grains. Through dynamic recrystallization, the initially coarse microstructure has been refined significantly. The absence of significant grain refinement at 1300°C and the lower strain rate of 10^{-5} sec^{-1} indicates that there is a delicate balance between the processes of grain refinement and grain coarsening at this temperature.

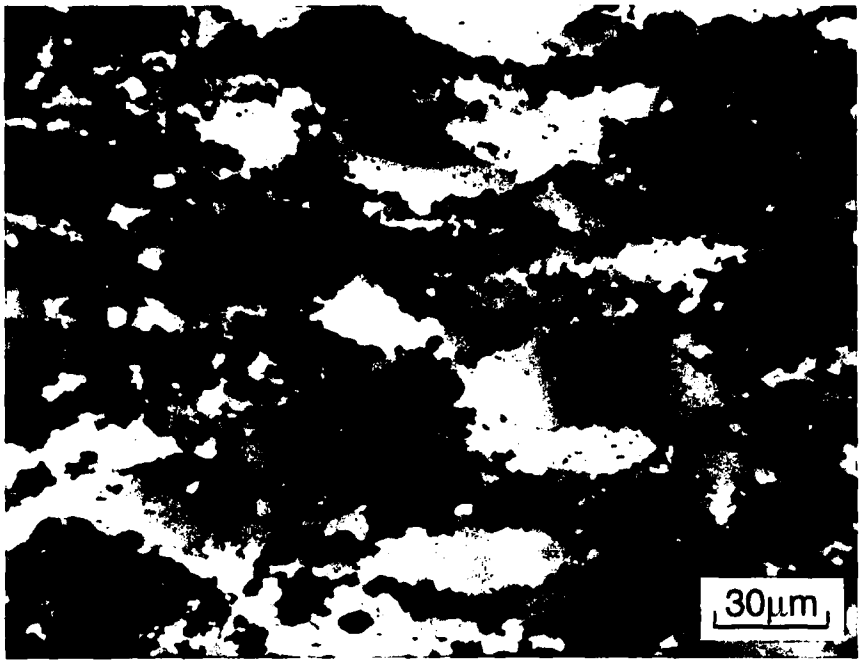

(a)

(b)

Fig. 15 Microstructure of $MoSi_2$ strained to 57.3% at 1300°C/$10^{-4}s^{-1}$ as revealed by (a) polarized light and (b) backscatter contrast in the SEM.

It would be very interesting to know the strength of fine grained, high purity $MoSi_2$. However, the high level of strain imparted to these samples resulted in significant barreling and intergranular separation throughout much of the volume of the compression sample. The micrographs of Fig. 14 were taken in the central region of the sample where grain boundary separation was minimal.

Conclusions

We have demonstrated that, with careful control of processing steps to avoid contamination, $MoSi_2$ can be made with a low silica content. As shown in Fig. 16, a consequence of this low silica content is a significant increase in the elevated temperature flow stress. The filled data points are our compression data at a strain rate of $10^{-4}s^{-1}$ on high purity and low purity material. The other materials on this plot were produced by mechanical alloying of elemental powders [17] and slip casting of commercial $MoSi_2$ powder [18]. Both materials were densified by hot pressing. Synthesis by $MoSi_2$ from elemental Mo and Si powders by mechanical alloying yields very low strength material. In our experience, MoSi2 produced by mechanical alloying contains very high levels of oxygen, > 1 wt% [6]. This translates into a very high volume fraction of SiO_2 particles and a resultant strength decrement. It is well-known that commercial MoSi2 powder contains significant levels of oxygen as SiO_2. Furthermore, slip casting, which produces a green body from a wet powder slurry, results in lower strengths [18] compared with dry handled powder [19] when both are hot pressed.

The higher strength of material with a low silica content could arise from two interrelated factors: grain size and silica content. The presence of a fine dispersion of silica particles limits the grain size of the impure material. The fine grain size coupled with viscous silica grain boundary films will enhance grain boundary sliding over dislocation motion in response to external stress. Deformation by grain boundary sliding will occur at stresses lower than those necessary to initiate dislocation glide+climb at high temperatures where the viscosity of the grain boundary silica is low.

From both direct observation and indirectly from analysis of the mechanical test data, we can conclude that deformation in high purity $MoSi_2$, at temperature in the range 1200°–1450°C and strain rates from 10^{-3}-$10^{-5}s^{-1}$, occurs by a combination of dislocation glide+climb and microcracking. Under purely compressive loading, the microcracking is transgranular, while tensile stresses result in intergranular crack formation. Recent work with single crystal $MoSi_2$ indicates that although it has a sufficient number of independent slip systems, the critical resolved shear stress necessary to activate the hardest orientations is extremely high at temperatures below ≈1300°C [11]. Five independent slip systems are required for the general shape change of a grain through dislocation glide. If either the cleavage strength or the intrinsic grain boundary strength is

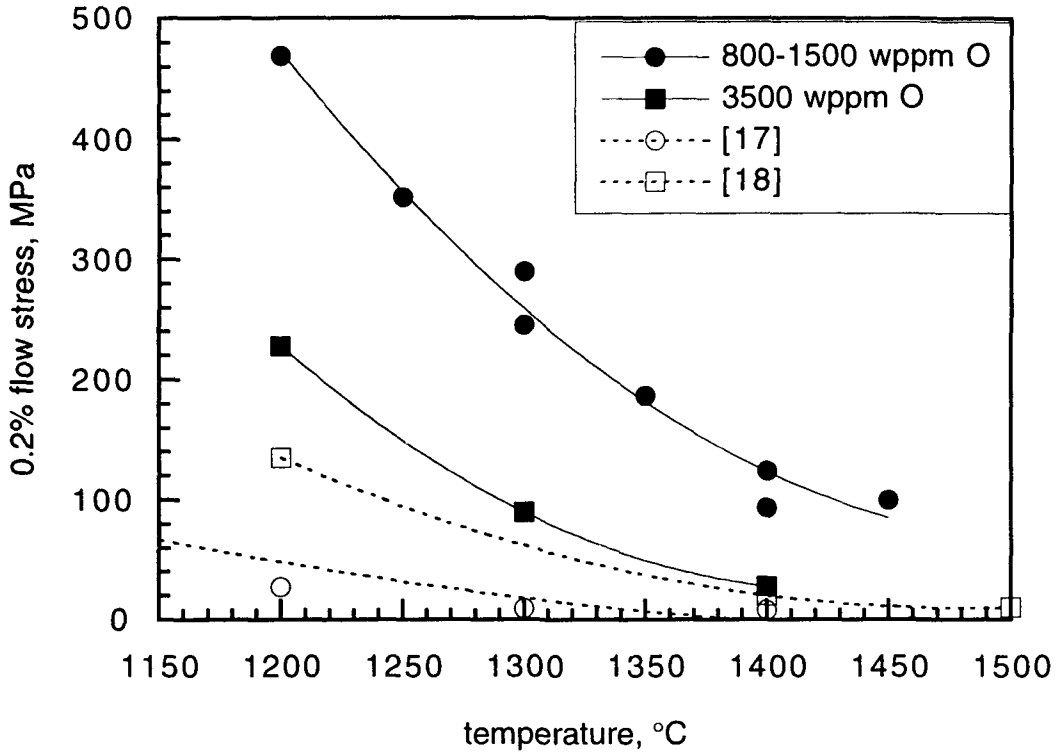

Fig. 16 Comparison of the flow stress values for $MoSi_2$ with various silica contents.

exceeded before sufficient slip systems can be activated, then microcracking will be favored over deformation as the mechanism of stress relief. The balance between the two mechanisms of dislocation glide+climb and microcracking will shift with temperature and strain rate; e.g., microcracking will be favored at lower temperatures and higher strain rates.

We have also shown that dynamic recrystallization leading to grain refinement can occur in $MoSi_2$ when it is "clean" enough; i.e., when it has a sufficiently low silica content that the principal deformation mechanism is not grain boundary sliding. However, the observation of dynamic recrystallization at 1300°C at a strain rate of $10^{-4}s^{-1}$ but not $10^{-5}s^{-1}$ indicates that the "window" for processing to finer grain sizes via dynamic recrystallization. is quite narrow. We observed that deformation at higher temperatures, ≥1400°C, invariably led to grain growth, even at the highest strain rate of $10^{-3}s^{-1}$. Higher strain rates and/or lower temperatures will increase the proportion of microcracking, effectively reducing the accumulation of deformation due to dislocation glide+climb and thus retarding or stopping completely the process of dynamic recrystallization.

References

1. P.J. Meschter and D.S. Schwartz, "Silicide-matrix materials for high-temperature applications", *JOM,* **4**(11) (1989), 52–55.

2. E.W. Lee, J. Cook, A. Khan, R. Mahapatra and J. Waldman, "The oxidation resistance of $MoSi_2$ composites ", *JOM* **43**(3) (1991), 54–57.

3. S.R. Srinivasen, R.B. Schwartz and J.D. Embury, "Ductile-to-brittle transition in $MoSi_2$", *Mat. Res. Soc. Symp.* Vol. 288, (1993) 1099–1104.

4. R.M. Aikin, Jr., "On the ductile-to-brittle transition temperature in $MoSi_2$", *Scripta Metall. Mater.* **26**, (1992) 1025–1030.

5. D.P. Mason and D.C. Van Aken, "The effect of microstructural scale on hardness of $MoSi_2$-Mo_5Si_3 eutectics", accepted for publication, *Scripta Met.*

6. D.A. Hardwick, P.L. Martin, S.N. Patankar and J.J. Lewandowski, "Processing-microstructure-property relationships in polycrystalline $MoSi_2$", *Proc. International Symposium on Structural Intermetallics,* (1993) 665–674.

7. D.A. Hardwick, "Composites based on molybdenum disilicide: progress and prospects", to be published in *Intermetallic Composites III,* MRS Spring '94.

8. B.H. Rabin and R.N. Wright, *Met. Trans.* **22A** (1991) 277.

9. A.K. Ghosh, A. Basu and H. Kung, "The effect of second phase properties on the compression creep behavior of $MoSi_2$ composites", *Mat. Res. Soc. Proc.* **273**, (1992) 259–266.

10. T. Hirano, N. Nakamura, K. Kimura and Y. Umakoshi, "Single crystal growth and mechanical properties of $MoSi_2$ and WSi_2", *Ceram. Eng. Sci. Proc.* **12**(9–10) (1991), 1619–1632.

11 S.A. Maloy, T.E. Mitchell, J.J. Petrovic, A.H. Heuer and J.J. Lewandowski to be published Proc. MRS Symposium *Silicides and Refractory Metals,* Fall 1993.

12. T.E. Mitchell, R.G. Castro, J.J. Petrovic, S.A. Maloy, O. Unal and M.M. Chadwick, "Dislocations, twins, grain boundaries and precipitates in $MoSi_2$", *Mater. Sci. Eng.* **A155** (1992) 241–249.

13. P.H. Boldt, J.D. Embury and G.C. Weatherly, "Room temperature microindentation of single crystal $MoSi_2$", *Mater. Sci. Eng.* **A155** (1992) 251–258.

14. H.J. McQueen and J.J. Jonas, "Recovery and recrystallization during high temperature deformation", in *Treatise on Materials Science,* Vol. 6, ed. R.J. Arsenault (1975) 394–493.

15. S. Bose, "Creep deformation in molybdenum disilicide", *Mat. Sci. Eng. A,* **A155** (1992) 217.

16. K. Sadananda, C.R. Feng and H. Jones, Mat. Sci. Eng. A, "Creep of $MoSi_2$ composites", **A155** (1992) 227.

17. R.B. Schwarz, S.R. Srinivasan, J.J. Petrovic and C.J. Maggiore, *Mat. Sci. Eng. A,* **A155** (1992) 75.

18. J.J. Petrovic and R.E. Honnell, *Ceramic Engineering and Science Proceedings,* **11** (7–8), 734 (1990).

19. C.H. Henager, Jr., J.L. Brimhall and J.P. Hirth, *Mat. Sci. Eng. A,* "Synthesis of $MoSi_2$-SiC composite in situ using a solid state displacement reaction", **A155** (1992) 109.

Publications and Presentations

"Synthesis of Molybdenum Disilicide from Elemental Powders": presentation at the First High Temperature Structural Silicides Workshop, Gaithersburg, MD, November 4–7, 1991.

"Synthesis of Molybdenum Disilicide from Elemental Powders": invited presentation at the University of Michigan, Ann Arbor, MI, November 8, 1991.

D.A. Hardwick, P.L. Martin and R.J. Moores, "Reaction synthesis of $MoSi_2$ from high purity elemental powders", *Scripta Metall. et Mater.*, **27**, (1992) 391–394.

D.A. Hardwick, "Clean Processing of Advanced Intermetallics", presentation at the AFOSR-ONR Workshop on Innovative Processing of Intermetallic Materials and Metal-Matrix Composites, May 1992.

"Molybdenum Disilicide: Ductility, Microcracking and Grain Boundary Silica": presentation at the 1993 High Temperature Materials Workshop, Wright Labs, Dayton, OH.

D.A. Hardwick, P.L. Martin, S.N. Patankar and J.J. Lewandowski, "Processing-microstructure-property relationships in polycrystalline $MoSi_2$", *Proc. International Symposium on Structural Intermetallics,* (1993) 665–674.

D.A. Hardwick and P.L. Martin, "Microcracking, Strain Rate and Large Strain Deformation Effects in Molybdenum Disilicide", MRS Proceedings: *Silicides and Refractory Metals,* Fall '93.

D.A. Hardwick, "Composites Based on Molybdenum Disilicide: Progress and Prospects", to be published in: Intermetallic Composites III, MRS Spring '94.

Appendix I

Processing-Microstructure-Property Relationships In Polycrystalline $MoSi_2$

D.A. Hardwick and P.L. Martin
Rockwell Science Center
Thousand Oaks, CA 91360

S.N. Patankar and J.J. Lewandowski
Department of Metals and Materials Science, Case Western Reserve University
Cleveland, OH 44106

(*Proceedings,* International Symposium on Structural Intermetallics, (1993) 665–674.)

PROCESSING-MICROSTRUCTURE-PROPERTY RELATIONSHIPS IN POLYCRYSTALLINE $MoSi_2$

D. A. Hardwick and P. L. Martin
Rockwell International Science Center,
Thousand Oaks.CA 91360

S. N. Patankar and J. J. Lewandowski
Dept. of Met. and Matls. Science, Case Western Reserve University,
Cleveland. OH 44106

Abstract

The influence of processing on the microstructure of polycrystalline, monolithic $MoSi_2$ is critically reviewed. Oxygen content, which often translates directly to glassy silica content, density and grain size are all important variables that are determined by the processing history. Each can exert a strong influence on subsequent material properties. Compressive strength and toughness results for well characterized, monolithic $MoSi_2$ produced by two different processing routes are presented. Both processing routes start from elemental powder; reaction-HIP synthesis produces a low oxygen, coarse grained material while mechanical alloying followed by hot-pressing yield a slightly more impure material but one with a very fine grain size. The results provide insight into the ongoing debate on the ductile-to-brittle transition temperature in $MoSi_2$.

Introduction

Molybdenum disilicide ($MoSi_2$) is an intermetallic compound that combines a high melting point (2020°C) with excellent resistance to high temperature oxidation (1,2). These attributes make it a candidate structural material for use at temperatures in the range of 1200° to 1600°C. At ambient and moderate temperatures $MoSi_2$ is brittle, but once the ductile-to-brittle transition temperature (DBTT) is exceeded, it rapidly loses strength. A number of composite designs (1) have been used to address the lack of low temperature toughness and high temperature creep resistance exhibited by $MoSi_2$. Significant increases in the low temperature fracture resistance of $MoSi_2$ have been obtained through ductile phase toughening (3-5). Approaches to increase the elevated temperature strength have included the addition of SiC whiskers (6), TiC particulates (7), a combination of SiC reinforcement and solid solution alloying with tungsten (8) and XD™ processing to introduce SiC, TiB_2, ZrB_2 or HfB_2 (9). These approaches to increasing the strength and toughness of $MoSi_2$ dictate a composite approach and thus will necessarily involve powder processing.

Although the formation of a silica layer on the surface of $MoSi_2$ is the key to its excellent high temperature oxidation resistance, the affinity of $MoSi_2$ for oxygen poses a variety of processing problems. SiO_2 or adsorbed oxygen will be present on the surface of $MoSi_2$ powder particles and will be incorporated into the consolidated monolithic or composite material. The silica particles in the consolidated product will be located at grain boundaries and triple points (10,11) and also within the grains. At temperatures below the glass transition temperature of SiO_2, T_g, such brittle particles could act as fracture nuclei, while viscous flow of the SiO_2 at higher temperatures could promote grain boundary sliding. The behavior of the silica may dominate the material response at very high concentrations of SiO_2, analogous to the dominant effect of sintering aids on the creep behavior in some ceramics (12).

The silica present in $MoSi_2$ is amorphous and therefore optically transparent; it can easily be mistaken for porosity in the optical microscope or the scanning electron microscope (SEM) as shown in Figure 1a. It is readily identified using reflected polarized light, as illustrated in Figure 1b, as the silica particles are strongly reflective.

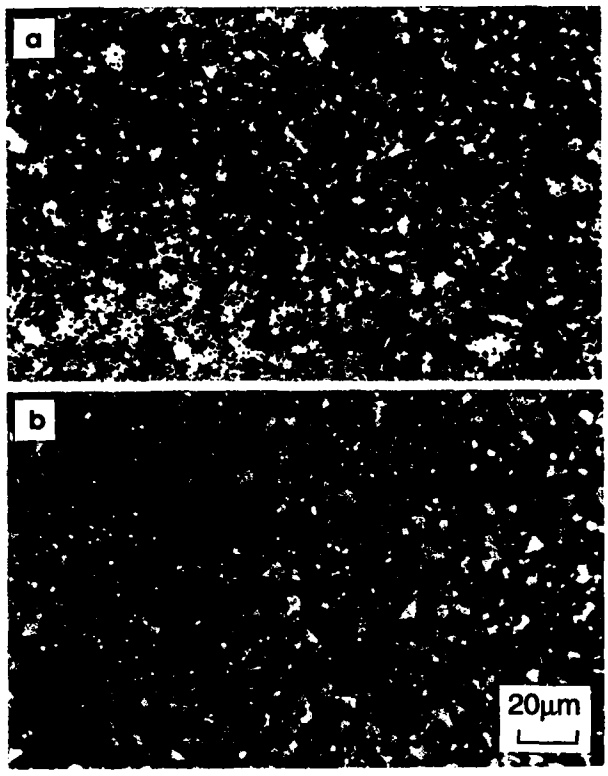

Figure 1: $MoSi_2$ viewed using a) backscattered electrons in the SEM and b) reflected polarized light.

The presence of SiO_2 at prior powder particle boundaries may also hinder grain growth, consistent with observations of a very fine grain size in monolithic $MoSi_2$ containing SiO_2. Cotton et al. (10) have produced monolithic $MoSi_2$ devoid of impurity phases via arc casting with a resulting grain size of 1mm. Subsequent hot pressing of powders obtained from pulverizing the arc cast material produced a material with a 5μm grain size and 5-10 vol% of a uniformly distributed second phase consisting of glassy silica and small amounts of Mo_5Si_3C. The carbon was not an intentional addition; it may have resulted from the use of graphite dies for hot pressing.

$MoSi_2$ powder is produced commercially by reacting Mo and Si in powder form. The sintered product is then milled to produce $MoSi_2$ powder and this powder usually contains significant amounts of silica. For example, vacuum hot pressed material produced from CERAC $MoSi_2$ powder contained 6500 wppm oxygen (13). Various methods for producing $MoSi_2$ have been explored as alternatives to the processing of commercially-available, impure powder. While the production of $MoSi_2$ from elemental powder precursors is an exothermic process, the energy to initiate this process can be supplied directly by heating the powder mixture or indirectly via mechanical work. The first route encompasses reaction synthesis and its variants such as self-propagating synthesis, combustion synthesis etc., while the second route is exemplified by mechanical alloying.

The synthesis of $MoSi_2$ by self-propagating synthesis has been extensively studied (14-16). When Mo and Si powders are mixed in accordance with the correct stoichiometry and heat is applied, single phase $MoSi_2$ results. The reaction is enhanced by increasing the density of the initial powder compact. When the elemental powders are reacted in a vacuum or inert gas environment, reaction synthesis is a self-purifying operation. Deevi (14) has reported producing $MoSi_2$ containing 2200 wppm oxygen from starting powders with much higher oxygen concentrations: 4700 wppm and 10,000 wppm oxygen in the Mo and Si respectively. Aikin (17) utilized reaction sintering in argon to produce $MoSi_2$ from nominal purity elemental powders. The sintered compact was crushed to a coarse -50 mesh powder, then consolidated by vacuum hot pressing followed by HIP'ing. The oxygen content of the resultant material was reported as 610 wppm.

The adiabatic temperature for the reaction of $MoSi_2$ from its constituent elements at room temperature has been calculated to be 1640°C (15). Raising the initial temperature of the reactants above room temperature will increase the adiabatic temperature until it equals the melting temperature of $MoSi_2$. Hardwick et al. (18) have demonstrated that the heat liberated by this exothermic reaction can be used to ensure a dense product when the exothermic reaction occurs under the conditions imposed by HIP processing. The resultant $MoSi_2$ was fully dense, despite the low HIP temperature of 1400°C. Given the high initial density of the powder compact achieved by cold isostatic pressing and a pre-heat temperature equal to the ignition temperature (determined as 1315°C by DTA measurements), the maximum temperature attained by the powder due to the exothermic reaction was probably equal to the melting temperature of $MoSi_2$. Incorporation of reaction synthesis into the final processing stage is obviously efficient as it eliminates several intermediate steps in the processing but there is a negative aspect; the reaction can no longer be used as a powder purification step. To overcome this limitation, Hardwick et al. (18) used very pure initial starting powders and performed all of their powder handling steps in a low oxygen, inert gas environment in an effort to limit SiO_2 contamination. These precautions resulted in a final (compacted) product containing 1600 wppm oxygen.

The use of mechanical alloying (MA) to produce $MoSi_2$ from elemental powders has also been extensively explored (19-23). Jayashankar and Kaufman (23) studied the phase evolution as a function of time for Mo+Si powders milled in an attritor. They found evidence of $\beta MoSi_2$* after just 0.5 hours of milling. With increased milling time the amount of $\beta MoSi_2$ increased and $\alpha MoSi_2$ also appeared. At very long milling times, Mo is still present b[illegible] the Si disappears, dissolving into the Mo and $MoSi_2$ phases. The disappearance of Si at long milling times has been confirmed by other investigations (20,21). Several investigators (21-23) have studied the phase evolution on heating of MA powders. Schwartz et al. (21) found only one exotherm in the range 500-600°C on heating their MA powder to 900°C that they attributed to complete transformation of all phases to the equilibrium α-$MoSi_2$. In contrast, Jayashankar and Kaufman (23) have more recently identified 3 exotherms in the temperature range RT to 1300°C and they were able to correlate these with various stages in the evolution of the equilibrium α-$MoSi_2$ phase.

Patankar et al. (22) investigated the initial stages of $MoSi_2$ formation in an MA powder produced by Spex milling of an elemental powder mixture. They found extensive $MoSi_2$ formation following 3 hours and 13 minutes of milling whereas powder examined after 3 hours and 12 minutes contained only traces of $MoSi_2$. Compound formation was accompanied by agglomeration of the MA powder, suggesting that the reaction was accompanied by considerable heat evolution. They postulated that self propagating high temperature synthesis was initiated in the powder once a critical level of stored energy was exceeded.

Consolidated material produced from MA powder may contain significant amounts of amorphous SiO_2 (23,25). Jayashankar and Kaufman (23) reported that hot-pressed $MoSi_2$ had approximately 15 vol% of second phase particles, mainly amorphous SiO_2. Assuming full density this corresponds to an oxygen content of 3.1wt% (8.9 at%); obviously an over-estimation if their material was not fully dense. As previously discussed, it is difficult to distinguish between porosity and glassy silica in reflected light micrographs or SEM micrographs. Schwartz et al. (21) claimed to

---

* Phase diagrams show that the tetragonal α–$MoSi_2$ is stable to 1900°C and transforms to the hexagonal β-$MoSi_2$ structure above this temperature. Boettinger et al (24) have shown that this high temperature polymorph should not exist in pure $MoSi_2$ but it may be stabilized by impurities or occur as a metastable phase, e.g. during rapid solidification.

have produced $MoSi_2$ with an oxygen content of 310 wppm, but the oxygen analysis technique used to obtain this result was not as reliable as more conventional techniques. In the analysis technique used by Schwartz et al. (21), the evolution of protons from bombardment of oxygen with deuterium ions was used to obtain the oxygen concentration; this method requires a calibration standard and Al_2O_3 (60 at% = 47wt% oxygen) was used. A more reliable analysis would result from the use of a standard closer in composition to the measured sample.

Several approaches have been developed to reduce or eliminate amorphous SiO_2 from the microstructure of $MoSi_2$ through the addition of elements that i) have a greater affinity for oxygen than Si and ii) form crystalline rather than amorphous second phases. Such second phases could then have a beneficial rather than a detrimental effect on the mechanical properties of the consolidated $MoSi_2$. Some investigators have focused on carbon additions to commercial $MoSi_2$ powder (11,25). During hot pressing, the principal reaction that occurs results in SiC formation and CO gas evolution. Some Mo_5Si_3C formation also occurs. In addition to CO, several other volatile species may be produced by reaction during the hot pressing operation, including MoO_3 and SiO. A complete analysis of the reaction products evolved during processing is provided elsewhere (26). Evolution of such gases during processing of C-containing material may produce some weight loss and porosity, although recent processing efforts on C-containing $MoSi_2$ have been successful in producing a fully dense product (27). Recently, Jayashankar and Kaufman (23) examined the carbothermic reduction of SiO_2 in MA mixtures of elemental Mo, Si and C. As discussed above, the binary material contained significant amounts of glassy silica phase but this C-containing material consisted of SiC, $MoSi_2$ and $(Mo,Fe)_{<5}Si_3C_{<1}$ (the Fe resulting from contamination from the milling medium) with negligible amounts of SiO_2.

With respect to the formation of more stable oxides than SiO_2, recent work by Gibala et al. (28) has demonstrated the deoxidizing effects of erbium additions to arc melted $MoSi_2$. As part of an investigation of $MoSi_2$-Mo_5Si_3 eutectics, Van Aken and Mason (29) prepared material from elemental Mo and Johnson Matthey $MoSi_2$ powder (3.61at% oxygen) with an addition of 0.35at% erbium. The powders were ball milled and then consolidated by hot pressing. This erbium-modified material contained $Er_2Mo_3Si_4$ but the silica, or more complex oxide, content of the material was not mentioned.

As the above review has shown, monolithic $MoSi_2$ has been produced by a variety of processing methods that result in material of variable quality with respect to such important parameters as stoichiometry, density, and silica content. As $MoSi_2$ is a line compound, small amounts of Mo_5Si_3 resulting from an Mo-rich stoichiometry are unavoidable, although they are preferable to the small amounts of Si that would accompany a Si-rich stoichiometry. Density determination allows qualitative measurement of the inherent porosity and provides a check of the quality of the consolidation operation. In general, material produced by HIP'ing has a higher density than material produced by hot pressing, but temperature is also an important processing variable. Finally, the oxygen content of the final product is obviously important as it relates directly to the volume fraction of glassy silica in the material. Each of these three factors will affect the mechanical properties of the final product at both ambient and elevated temperatures.

The mechanical properties of polycrystalline $MoSi_2$ have been considered to fall within one of three regimes (1): (a) $T < 925°C$: strong + brittle; (b) $925°C < T < 1250°C$: strong + "ductile" and (c) $T > 1250°C$: weak + ductile. However, debate has recently arisen concerning the ductile-to-brittle transition temperature (DBTT) of $MoSi_2$ (17, 30-32). Values as low as 950°C (31) and as high as between 1300° and 1400°C (17) have been reported. The influence of glassy silica on the DBTT is also under discussion with claims that it has no influence on the DBTT (17) and counterclaims that the DBTT is decreased in the presence of SiO_2 (30).

While the DBTT continues to receive considerable attention, less work has been done on the high temperature toughness properties of monolithic $MoSi_2$. Recently, Maloy et al. (11, 24) and Patankar et al (32) investigated the hardness, indentation toughness, and notched toughness behavior of $MoSi_2$ produced via a variety of methods. The notch toughness of $MoSi_2$ prepared from CERAC powders decreased with increasing temperature over the range 800 - 1400°C and the fracture mode at the high temperatures was predominantly intergranular (11). De-oxidizing with C (11,25) produced a material with significantly greater elevated temperature hardness and notch toughness and in this material the fracture mode was predominantly transgranular. Identical studies were performed on $MoSi_2$ produced via MA followed by vacuum hot pressing (32); the hardness of the MA material exceeded that of both the material produced from the CERAC powders and the C-containing material.

The present investigation was undertaken to provide additional information on the deformation behavior of $MoSi_2$ in well-characterized materials. Right circular cylinders of $MoSi_2$, produced by reaction HIP synthesis, have been compressed to stresses well past the yield stress at various temperatures and strain rates. Relatively little work has focused on the effects of strain rate on the properties of $MoSi_2$, although it is likely to influence both the high temperature flow and fracture behavior. The relative contributions of microcracking and grain deformation to the total strain have been assessed by careful observation of the deformed microstructures. In a complementary study, $MoSi_2$ fabricated via MA and subsequently vacuum hot pressed, has been tested to determine both the smooth bend and notch toughness behavior over a range of temperatures. Additional smooth bend experiments were conducted on materials prepared by Aikin (17) for comparison with the results obtained MA materials.

Experimental Procedure

Compression Testing

The $MoSi_2$ used in the compression testing was produced by reaction synthesis during HIP processing. High purity powders of molybdenum (600 wppm oxygen) and silicon (20 wppm oxygen) in the correct weight ratio to ensure stoichiometric $MoSi_2$ were ball

milled in vacuum to ensure an intimate mixture of the powders. The powder mixture was cold isostatically pressed at 200 MPa for 30 minutes. The CIP preform was lathe turned prior to its placement within cylindrical Ta HIP cans that were evacuated at 350°C prior to sealing. All of the powder handling steps were done in a low oxygen, inert gas environment to limit oxygen exposure and reduce SiO_2 contamination. HIP'ing was carried out at 200 MPa and a maximum furnace temperature of 1400°C. More complete details of the processing have been published elsewhere (18). Right circular cylinders for compression testing were electro-discharge-machined from the HIP compacts; a diameter of an average cylinder was 9.5mm and the length was 10mm. The ends of the cylinders were polished flat and perpendicular to the cylinder axis. Compression testing was performed over a range of strain rates from $1x10^{-3}$ to $1x10^{-5}$ sec^{-1}. All testing was conducted in a vacuum of $5x10^{-3}$ Pa or better and at temperatures in the range 1200° to 1400°C. The compression platens were silicon nitride and the specimens were lubricated with boron nitride to reduce frictional effects. After testing, the cylinders were sectioned vertically and the microstructures examined optically and in the SEM.

Bend Testing and Hot Hardness

The $MoSi_2$ for bend testing was produced by mechanical alloying using a Spex mill/model 8000 in the manner described elsewhere (22). The resulting silicide powders were degassed at 800°C for 6 hours prior to hot pressing at 1500°C for 30 minutes at a pressure of 51.7 MPa. Toughness was measured directly using notched four point bend bars and indirectly from microhardness measurements made with a Nikon hot hardness testing machine. Smooth bars were also tested in four point bending. The dimensions of the smooth bend bars were 25 mm x 2 mm x 2.5 mm, while that of the notched specimens were 25 mm x 2 mm x 5 mm. The notches were placed in the specimens via a slow speed diamond blade and the notch root radius was approximately 100 µm. All bend tests were conducted in four point bending on a Model 810 MTS machine operated under displacement control at temperatures ranging from 800 - 1400 C. The displacement rate for the notched bend tests was 50 µm/min, while that for the smooth bend tests was 127 µm/min.

Experimental Results

Compression Testing

The reaction synthesized $MoSi_2$ after HIP processing contained 1000-2000 wppm oxygen, as determined by standard vacuum fusion techniques, and was fully dense. Figure 2 shows that the microstructure of $MoSi_2$ prior to compression testing had an average grain size of 40µm. The silica particles (i.e. the bright white dots in Figure 2) are randomly distributed in the microstructure while a small volume fraction of Mo_5Si_3 is found at $MoSi_2$ grain boundaries and triple points.

The 0.2% offset compressive yield stress as a function of temperature and strain rate is plotted in Figure 3. Lines are drawn through the data at the lower strain rates to facilitate data interpretation. Also shown on this plot is data obtained by Aikin (17) on testing $MoSi_2$ with an average grain size of 20µm at a compressive strain rate of $7x10^{-5}$. A comparison of the data of Aikin (17) with the current data set obtained at $1x10^{-4}$ reveals that the current material has comparable flow stress at 1200°C but has lower strength at higher temperatures. This difference may be due to SiO_2 content and/or grain size; Aikin (17) reported an oxygen content of 610 wppm and while the average grain of his material was 20µm, grains with diameters of 100µm and larger were also present.

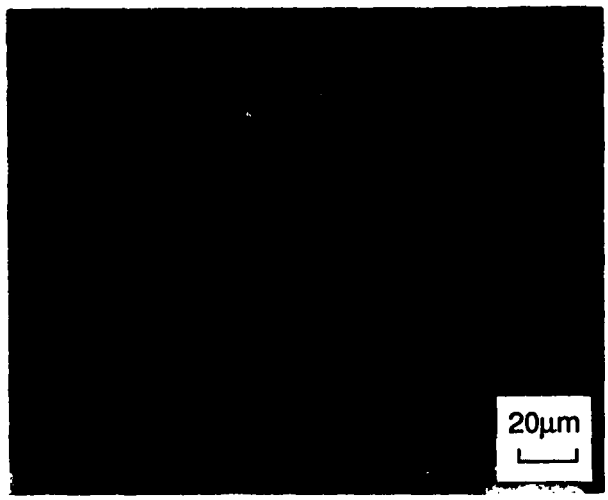

Figure 2: Microstructure of $MoSi_2$ produced by reaction HIP processing from elemental powders.

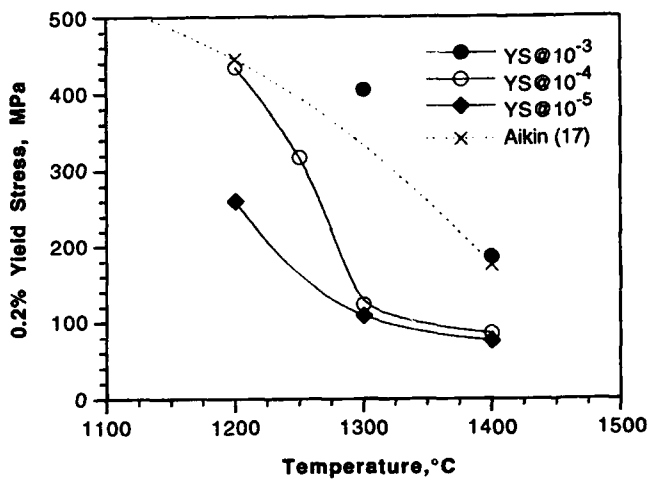

Figure 3: Compressive stress at 0.2% strain as a function of temperature and strain rate.

All of the tests were terminated at strains greater than 1% (all strain values are plastic), the lowest being 1.4% strain in the specimen tested at 1200°C and a strain rate of $1x10^{-4}$ sec^{-1}. The majority of the tests were terminated at strains of 5-6% but some were allowed to proceed to higher strains: 13% for the specimen tested at 1400°C and $1x10^{-4}$ sec^{-1} and 15.2% for the specimen tested at 1300°C and $1x10^{-4}$ sec^{-1}.

None of the samples exhibited cracking on the external surfaces but metallographic examination of samples sectioned longitudinally revealed that all of the samples contained various amounts of internal microcracks. These cracks were transgranular in nature, each traversing one or two grains before stopping. Figure 4 shows microcracking in the specimen tested to 6.6% strain at $1x10^{-5}$ sec^{-1} at 1400°C, the lowest strain rate and highest temperature. This microstructure also shows evidence of grain growth compared with the starting microstructure shown in Figure 2. In addition to the microcracking, specimens tested to higher strains exhibited grain boundary separation in the barreled region of the specimens, presumably due to the tensile component of stress in those regions.

Figure 4: Microcracking in $MoSi_2$ tested to 6.6% strain at $1x10^{-5}$ sec^{-1} at 1400°C.

To determine the strain rate sensitivity of the operative deformation processes, the stress-strain data has been plotted on a log σ - log $\dot{\varepsilon}$ basis as shown in Figure 5. The upward curvature indicated by this plot indicates an increase in the strain rate sensitivity or "m" value.

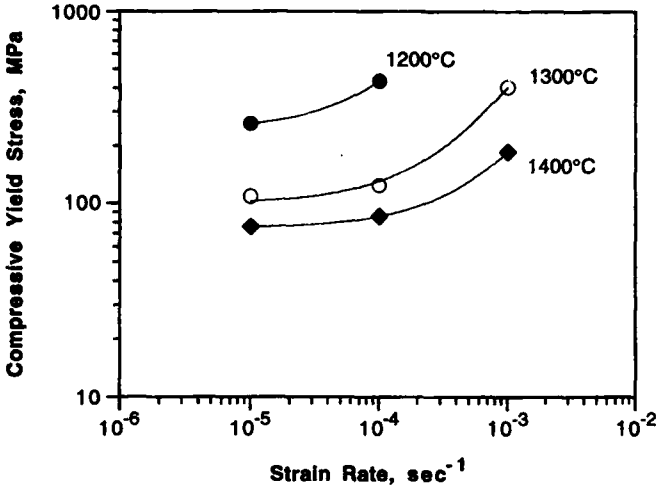

Figure 5: Strain rate sensivity plot from compression data for $MoSi_2$.

Bend Testing and Hot Hardness

The MA-synthesized $MoSi_2$ after hot pressing contained 1.2wt% oxygen, as determined by standard vacuum fusion techniques. The material had an average grain size of 1-5μm as illustrated in Figure 6.

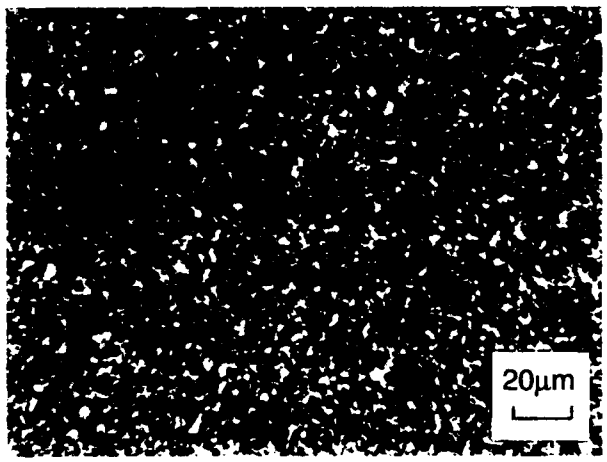

Figure 6: Microstructure of $MoSi_2$ produced by MA of elemental powders followed by hot pressing.

Variation of the hardness of $MoSi_2$ as a function of temperature is shown in Figure 7. Also included in Figure 7 are results obtained on $MoSi_2$ prepared from CERAC powder, as well as results obtained on C-containing materials reported previously. (10,25) The MA material exhibited hardnesses in excess of the C-containing material at all temperatures.

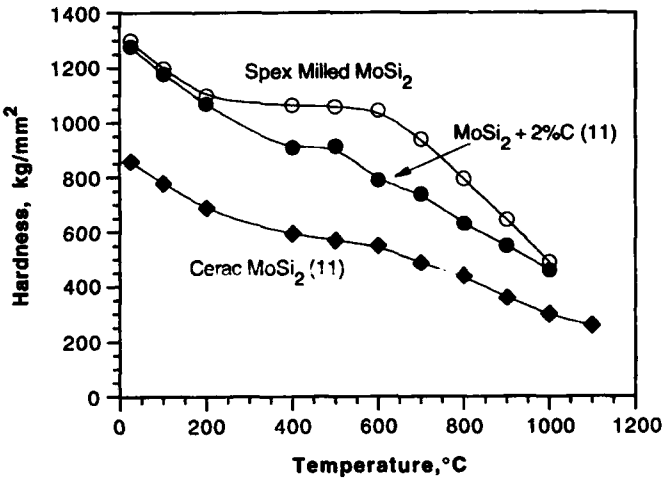

Figure 7: Hardness of $MoSi_2$ produced by various processing routes as a function of temperature.

Toughness values for the MA $MoSi_2$ were computed from this hardness data using the method of Evans and Charles (33) and these are shown in Figure 8. The toughness values obtained from the indentation cracks were nearly constant to 800°C, and then increased at higher test temperatures.

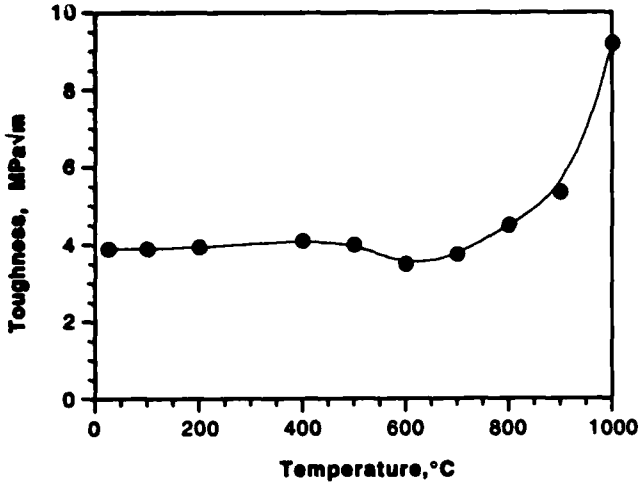

Figure 8: Toughness of MA-synthesized, hot-pressed $MoSi_2$ calculated from indentation hardness results.

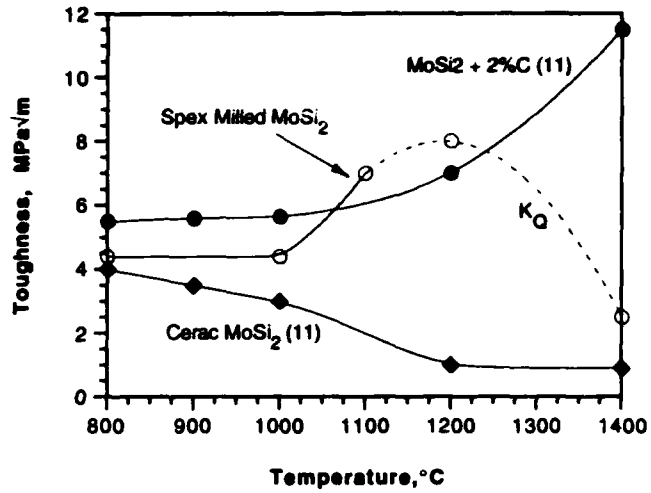

Figure 9: Toughness as a function of temperature obtained from notched bend tests on $MoSi_2$ produced by various processing routes

The smooth bend behavior of the MA materials is summarized in Table I which summarizes both fracture stresses and material behavior.

Table I Smooth Bend Data on $MoSi_2$

Material	Test Temperature	Fracture Stress	Yield Stress
MA	900 C	250 MPa	*
MA	1000 C	245 MPa	*
MA	1100 C	> 380 MPa	180 MPa
Aikin $MoSi_2$	1200 C	250 MPa	*
Aikin (17)	1200 C	250 MPa	*
Aikin (17)	1400 C	250 MPa	180 MPa (c)

* - did not yield prior to fracture (c) - compression test

The MA materials fractured in the linear portion of the load vs. displacement traces up to 1000°C. Significant non-linearity was obtained at 1100°C in the MA material. The material supplied by Aikin (17) was tested at 1200°C and failed in the linear portion of the load vs. elongation trace. The calculated fracture stresses for both the MA material and the material supplied by Aikin (17) are similar to those already reported by Aikin (17), as summarized in Table I. The main difference between the present work and the work by Aikin (17) is the apparent lower DBTT in the MA material. The yield stress calculated from bend testing at 1100°C for the MA material was also somewhat lower than that obtained in the compression tests conducted on reaction synthesized materials as well as those reported by Aikin (17) but much higher than that reported by Schwartz et al.(30).

Figure 9 shows the notched four point bend toughness as a function of temperature for the same materials shown in Figure 8. In contrast to the CERAC powders and similar to the C-containing material (10,25), the toughness of the Spex-milled $MoSi_2$ remained roughly constant from 800° - 1000°C.

The toughness of the material prepared with CERAC powder decreased at higher temperatures, while that of both the MA and C-containing materials increased with increasing temperature to 1200°C. It should be noted that the notched specimens exhibited linear load vs. displacement traces at temperatures up to 1100°C, but significant non-linearity and evidence of notch-root plasticity at temperatures of 1200°C and above. At 1400°C, extensive deformation occurred in the notched bend specimen and there was no evidence of large scale fracture. The apparent decrease in the toughness of the Spex-milled material at 1400°C was a consequence of the low yield strength at that temperature. Although significant non-linearity was obtained, the load-carrying capacity of this material was low, resulting in a low toughness. At all test temperatures, the fracture surfaces of the MA-synthesized $MoSi_2$ exhibited a mixture of intergranular and transgranular failure.

Discussion

The observation of transgranular microcracks in material tested at even the highest temperature and lowest strain rate is probably the single most significant point arising from the compression testing in the current investigation. The only other reported incidence of stable, transgranular microcracks was in the work of Maloy et al. (25) where transgranular micro-cracking and a non-linear load vs. displacement trace was obtained in C-containing material tested in notched bending at 1400°C. The majority of previous investigators have not reported microcracking; in impure, high silica material, microcracking may not occur as the stress would be dissipated through viscous sliding of the grain boundary silica film before the critical stress to nucleate transgranular cracks could be achieved. The microcracking was not reflected in the recorded stress-strain curves; these curves exhibited the usual non-linearity associated with normal plasticity. These microcracks extended over 1 to 2 grains only. In a study involving high purity single crystals of $MoSi_2$, Hirano et al. (34) found a large variation in the critical resolved shear stress (CRSS) for glide, indicating that some orientations were

more amenable to slip than others. If, as would be expected, the HIP-synthesized $MoSi_2$ had a random crystallographic texture, then "soft" grains would be randomly interspersed with "hard" grains. Cracks could nucleate from stress concentrations at grain boundaries, then propagate unchecked through 1 or 2 neighboring "hard" oriented grains before being blunted or stopped in "soft" grains through the operation of dislocation glide processes. The observation of very non-uniform dislocation densities in strained $MoSi_2$, with dislocation-free grains adjoining dislocation-rich grains is consistent with this mechanism (35). In addition, it has been shown that plastic flow itself can initiate cracking in $MoSi_2$ (36). Atomically sharp cracks were observed in the region of severe strain gradient under hardness indentations; further work will be necessary to show whether this is a general mechanism or is peculiar to the complex stress field under the indenter. Due to the compressive stress state used in the present experiments, the contribution of the displacement provided by these cracks to the total strain is difficult to determine. No evidence of shear strain was observed metallographically around the microcracks, indicating that their strain contribution was probably small and that the cracks were probably closed under stress.

The strain rate sensitivity plot, Figure 5, indicates that deformation in polycrystalline $MoSi_2$ at 1300° or 1400°C is unaffected by low strain rates but becomes rate dependent at lower temperatures or (equivalently) higher strain rates. Similar results were found by Hirano et al. (34) in their experiments with single crystal $MoSi_2$. Their single crystal data showed that a 100MPa strength increase accompanied a decade increase in strain rate. Again, interpretation of the polycrystalline data is complicated by the observation of the microcracking. More work is obviously required to determine the exact deformation mechanism(s), through a better understanding of the effects of grain size, temperature, stress state and strain rate.

It is clear that discussion continues to focus on the ductile-to-brittle transition of $MoSi_2$ (17,30,32). Observations to date reveal that there appears to be both a temperature and strain rate dependence of the flow and fracture behavior of this material, somewhat analogous to that exhibited by bcc metals. In the case of bcc materials, it has been clearly demonstrated that changes in grain size, interstitial content, stress state, strain rate, and alloy content can exert a large influence on the ductile-to-brittle transition temperature. (37) For example, in the literature on ferrous structural materials (e.g. steels containing carbide particles), it has been demonstrated that the yield stress is controlled by such factors as the test temperature, grain size, and the size/spacing of the carbide particles, while the cleavage fracture stress is generally assumed to be temperature independent, yet strongly dependent on the grain size and the details of the carbide particles (e.g. size), as reviewed recently by Thompson and Knott (38). A decrease in the grain size and/or carbide size generally produces an decrease in the ductile-to-brittle transition temperature. (37). This arises from the greater increase in the cleavage fracture stress afforded by finer grains and/or finer carbide sizes in comparison to the increase in the yield strength arising from those same microstructural changes. Such effects have been documented in a variety of steels with simple ferrite/carbide microstructures (37-41) as well as in more complicated microstructures such as pearlitic steels (42,43). This approach has recently been applied to TiAl and an alloy of the intermetallic Ti_3Al (44).

While it would be appealing to consider a similar scenario for the fracture of $MoSi_2$, an additional complicating factor is the presence of SiO_2 in this material. As previously mentioned, the SiO_2 particles could act as flaw nuclei at low temperatures (e.g. below T_g of SiO_2), as it is likely that the surface energy/toughness of the silica is less than that of $MoSi_2$ at low temperatures. Similar observations on the detrimental effects of brittle inclusions on the ductility of intermetalllics have also been reported (45). The behavior at higher temperatures is also complicated by the presence of SiO_2. While non-linearity and ductility in ferrous based materials are typically associated with dislocation plasticity, the presence of SiO_2 in $MoSi_2$ may promote non-linearity due to softening of the SiO_2 at elevated temperatures. Thus, the mere appearance of non-linearity may not be indicative of true plasticity. In addition, comparison between the data obtained by different researchers working on the ductile-to-brittle transition temperature must be approached with some caution, as the test conditions may not be identical between investigators. For example, differences in grain size, silica content, and strain rate could easily account for the differences reported in the literature. Caution must also be exercised in the interpretation of fracture surface features with the above points in mind. For example, the presence of grain boundary silica may promote intergranular fracture at high temperatures due to the preferential, weak (i.e. low strength) path that is provided by the viscous silica. However, transgranular fracture may also be observed in such systems, particularly at large grain sizes. To continue the analogy with ferrous materials, it is well known that in these materials the cleavage fracture stress is grain size dependent and that transgranular fracture may occur despite the presence of weak grain boundaries in such systems (46). Thus, the failure processes in such materials should be viewed as a competition between yielding and brittle fracture, in which the operative fracture path may depend sensitively on the variables listed above.

In the present work on $MoSi_2$, transgranular microcracks were observed during compression testing, as shown in Figure 4, while a mixture of intergranular and transgranular fractures have been reported by a variety of other researchers (10,17,25,30) on bend testing of materials with different grain sizes, compositions and alloying additions. When all of these different factors are taken into account, these various results may indeed be self-consistent. In order to resolve the inconsistencies present among the results presented in the literature, particular attention must be paid in future investigations to the pertinent microstructural variables of grain size and SiO_2 content as well as test parameters such as temperature and strain rate. In particular, the source of any observed non-linearities encountered during testing should be thoroughly investigated and not arbitrarily assigned to plastic flow. The sources of the ductile-to-brittle transition in $MoSi_2$, and in other intermetallics and silicides, warrant continued scrutiny and careful investigations will be essential for understanding the behavior of these materials.

Acknowledgments

The work performed at the Rockwell Science Center was supported by AFOSR, Contract No. F49620-91-C-0027. Work performed at the Case School of Engineering, CWRU was supported by AFOSR Contract No. 89-0508 and by DARPA-ONR Contract No. N-00014-86-K-0773.

References

1. P. J. Meschter and D. S. Schwartz, "Silicide-matrix materials for high-temperature applications", JOM, 4(11) (1989), 52- 55.

2. E. W. Lee, J. Cook, A. Khan, R. Mahapatra and J. Waldman, "The oxidation resistance of $MoSi_2$ composites ", JOM 43(3) (1991), 54-57.

3. E. Fitzer and W. Remmele,"Possibilities and limits of metal reinforced refractory silicides especially molybdenum disilicide", Proc. 5th Int. Conf on Composite Materials, ICCM-V, ed. W. C. Harrigan, Jr, J.Strife and A. K. Dhingra, pp 515-530, AIME, Warrendale, PA (1985).

4. T. C. Lu, A. G. Evans, R. G. Hecht and R. Mehrabian, "Toughening of $MoSi_2$ with a ductile (niobium) reinforcement" Acta Met. Mater. 39, (1991) 1853-1862.

5. L. Xiao and R. Abbaschian,"The role of matrix/reinforcement interfaces in the fracture toughness of ductile phase reinforced $MoSi_2$ composites", Metall. Trans. 23A, (1992) 2863-2872.

6. W. S. Gibbs, J. J. Petrovic and R. E. Honnell,"SiC whisker-$MoSi_2$ matrix composites" Ceram. Eng. Sci. Proc. 8, (1987) 645-648.

7. J-M. Yang, W. Kai and S. M. Jeng,"Development of TiC particle-reinforced $MoSi_2$ composite", Scripta Metall. Mater. 23 (1989) 1953-1958.

8. J. J. Petrovic and R. E. Honnell,"SiC reinforced-$MoSi_2$/WSi_2 alloy matrix composites", Ceram. Eng. Sci. Proc. 11 (1990) 734-744.

9. R. M. Aikin, Jr,"Strengthening of discontinuously reinforced $MoSi_2$ composites at high temperatures", Mater. Sci. Eng. A155 (1992) 121-133.

10. J. D. Cotton, Y. S. Kim and M. J. Kaufmann, "Intrinsic second-phase particles in powder-processed $MoSi_2$", Mater. Sci. Eng., A144, (1991) 287-291.

11. S. Maloy, A. H Heuer, J. J. Lewandowski and J. J. Petrovic,"Carbon additions to molybdenum disilicide: improved high temperature mechanical properties", J. Am. Ceram. Soc., 74(10), (1991) 2704-2706 .

12. D. W. Richerson, "Effect of impurities on the high temperature properties of hot-pressed silicon nitride", Amer. Ceram. Soc. Bull., 52(7), (1973) 560-562, 569.

13. R. M. Aikin, Jr, "Structure and properties of in situ reinforced $MoSi_2$," Ceram. Eng. Sci. Proc. 12(9-10) (1991), 1643-1655.

14. S. C. Deevi, "Self-propogating high temperature synthesis of molybdenum disilicide", J. Mat. Sci., 26, (1991) 3343-3353.

15. S. Zhang and Z. A. Munir, "Synthesis of molybdenum silicides by the self-propagating combustion method", J. Mat. Sci., 26, (1991) 3685-3688.

16. S. C. Deevi, "Diffusional reactions in the combustion synthesis of MoSi2", Mater. Sci. Eng. A149 (1992) 241-251.

17. R. M. Aikin, Jr, "On the ductile-to-brittle transition temperature in $MoSi_2$", Scripta Metall. Mater. 26, (1992) 1025-1030.

18. D.A. Hardwick, P.L. Martin and R.J. Moores, "Reaction synthesis of $MoSi_2$ from high purity elemental powders", Scripta Metall. Mater., 27, (1992) 391-394.

19. Y. S. Kim, M. R. Johnson, R. Abbaschian and M. J. Kaufman, "Effect of Ceramic Dispersoids on the High Temperature Strength of Mechanically Alloyed $MoSi_2$", Mat. Res. Soc. Symp. Vol. 213, (1991) 839-845.

20. S. R. Srinivasen and R. B. Schwartz, "Synthesis of $MoSi_2$-based alloys by mechanical alloying", in "Novel Powder Processing", Advances in Powder Metallurgy and Particulate Materials - 1992, Vol. 7, published by Metal Powder Industries Federation, Princeton, NJ, pp 345-358.

21. R. B. Schwartz, S. R. Srinivasen, J. J. Petrovic and C. J. Maggiore, "Synthesis of molybdenum disilicide by mechanical alloying", Mater. Sci. Eng., A155 (1992) 75-83.

22. S. N. Patankar, S-Q. Xiao, J. J. Lewandowski and A. H. Heuer, "The mechanism of mechanical alloying of $MoSi_2$", to be published J. Mater. Res. 8(6), (1993).

23. S. Jayashankar and M. J. Kaufman, "Tailored $MoSi_2$/SiC composites by mechanical alloying", to be published in J. Mater. Res. 8(6), (1993).

24. W. J. Boettinger, J. H. Perepezko and P. S. Frankwicz, "Application of ternary phase diagrams to the development of $MoSi_2$-based materials", Mater. Sci. Eng. A155 (1992) 33-44.

25. S. Maloy, J. J. Lewandowski and A. H. Heuer, "Effects of carbon additions on the high temperature mechanical properties of molybdenum disilicide ", Mater. Sci. Eng., A155, (1992) 159-163.

26. N. Jacobson, K. Lee, S. A. Malloy and A. H. Heuer, "Chemical reactions in processing of $MoSi_2$ + carbon powders", J. Amer. Ceram. Soc. (1993) in press.

27. S. N. Patankar, J. J. Lewandowski, and A. H. Heuer, unpublished research, CWRU, 1993.

28. R. Gibala, A. K. Ghosh, D. C. Van Aken, D. J. Srolovitz, A. Basu, H. Chang, D. P. Mason and W. Yang, "Mechanical behavior and interface design of $MoSi_2$-based alloys and composites", Mater. Sci. and Eng., A155, (1992) 147-158.

29. D. P. Mason and D. C. Van Aken, "The effect of microstructural scale on hardness of $MoSi_2$-Mo_5Si_3 eutectics", accepted for publication, Scripta Met.

30. S. R. Srinivasen, R. B. Schwartz and J. D. Embury, "Ductile-to-brittle transition in $MoSi_2$", Mat. Res. Soc. Symp. Vol. 288, (1993) 1099-1104.

31. J. Schlichting, "Molybdenum disilicide as component of modern high temperature composites", High Temperatures-High Pressures, 10(3), (1978) 241-269.

32. S. N. Patankar and J. J. Lewandowski, "Effect of processing on the high temperature mechanical properties of $MoSi_2$", Mat. Res. Soc. Symp. Vol. 288, (1993) 829-834.

33. A. G. Evans and E. A. Charles,"Fracture toughness determinations by indentation", J. Amer. Ceram Soc., 59 (1976) 371-372.

34. T. Hirano et al., "Single crystal growth and mechanical properties of $MoSi_2$ and WSi_2", Ceram. Eng. Sci. Proc. 12(9-10) (1991), 1619-1632.

35. T. E. Mitchell, R. G. Castro, J. J. Petrovic, S. A. Maloy, O. Unal and M. M. Chadwick, "Dislocations, twins, grain boundaries and precipitates in $MoSi_2$", Mater. Sci. Eng. A155 (1992) 241-249.

36. P. H. Boldt, J. D. Embury and G. C. Weatherly, "Room temperature microindentation of single crystal $MoSi_2$" Mater. Sci. Eng. A155 (1992) 251-258.

37. J. F. Knott, "Fundamentals of Fracture Mechanics", Butterworths, 1973.

38. A.W. Thompson and J.F. Knott, "Micromechanisms of brittle fracture", Metall. Trans. A, 24A (1993) 523-534.

39. J.F. Knott, "On the ductile-to-brittle transition in steel", J. Iron and Steel Inst. 205 (1967) 288-291.

40. D. A. Curry and J. F. Knott, "Effects of microstructure on cleavage fracture stress in steel", Metal Science J., 12 (1978) 511-514.

41. D. E. McRobie and J.F. Knott, "Effects of strain and strain aging on fracture toughness of C-Mn weld metal", Materials Science and Technology, 1 (1985) 357-365.

42. J.J. Lewandowski and A.W. Thompson,"Microstructural effects on the cleavage fracture stress of fully pearlitic steel", Metall. Trans. A, 17A (1986) 1769-1786.

43. J.J. Lewandowski and A.W. Thompson,"Micromechanisms of cleavage fracture stress of fully pearlitic microstructures", Acta Metall. Mater. (1987) 1453-1462.

44. A. W. Thompson, "Environmental Effects in Titanium Aluminide Alloys", presented at Symposium on "Environmental Effects in Advanced Materials", TMS Fall Meeting, Detroit, 1990.

45. W.R. Kerr, "Fracture of Fe_3Al", Metall Trans. A, 17A (1986) 2298-2300.

46. J.J. Lewandowski, C. A. Hippsley, M. B. D. Ellis and J.F. Knott,"Effects of impurity segregation on sustained load cracking of $2^1/_4$ Cr-1Mo Steels", Acta Metall. Mater., 35 (1987) 593-608.

Appendix II

Composites Based On Molybdenum Disilicide: Progress And Prospects

D.A. Hardwick
Rockwell Science Center
Thousand Oaks, CA 91360

(to be published in: *Intermetallic Composites III*, MRS Spring '94)

COMPOSITES BASED ON MOLYBDENUM DISILICIDE: PROGRESS AND PROSPECTS

D. A. HARDWICK
Rockwell Science Center, 1049 Camino Dos Rios, Thousand Oaks, CA 91360

Abstract

As the temperature demands increase in advanced aerospace systems, engineering materials that can withstand 1200° to 1600°C exposure in air must be developed. $MoSi_2$ is an intermetallic compound that has many, though not all, of the necessary physical and mechanical properties for use in this temperature regime. At ambient and moderate temperatures $MoSi_2$ is brittle, but once the ductile-to-brittle transition temperature (DBTT) is exceeded, it rapidly loses strength. Recent progress in, and current status of, the research efforts in $MoSi_2$ matrix composites will be reviewed, with an emphasis on the critical issues that currently impede progress to application.

Introduction

Well-known as a heating element material (1), $MoSi_2$ was first examined for structural use by NACA (predecessor to NASA) by Maxwell (2,3) and Long (4). This early work centered on the production of $MoSi_2$ powders, that were then densified by uniaxial hot pressing. In addition to hot tensile and stress rupture testing, turbine blade shapes were subjected to thermal shock tests. Maxwell and Long found that $MoSi_2$ was very brittle at temperatures below 1000°C with monotonically increasing ductility and decreasing strength at temperatures above 1000°C.

Over the years, a number of composite designs have been used to address the lack of low temperature toughness and high temperature creep resistance exhibited by $MoSi_2$. Attempts to improve the low temperature mechanical properties have relied extensively on two major approaches to composite toughening, namely brittle fiber pull-out and ductile fiber fracture. Approaches to increase the elevated temperature strength have included the addition of ceramic whiskers or particulates and solid solution alloying. Ductile phase toughening of $MoSi_2$ was first investigated by Fitzer, who incorporated refractory metal wires into a $MoSi_2$ matrix (5-7). The refractory metals are not in thermodynamic equilibirum with $MoSi_2$ at any temperature and Fitzer established the parabolic rate constants for interdiffusion and conversion to the R_5Si_3 compounds (R=refractory metal). Work on ductile fiber toughening has continued with emphasis on coatings to limit interdiffusion and examination of alternate ductile reinforcement morphologies including particles and layers. Research has also focussed on $MoSi_2$ composites

reinforced with ceramic whiskers or particulates. Many potential carbide, nitride, oxide and boride ceramic reinforcements are known to be thermodynamically stable in $MoSi_2$, including SiC, TiC, Si_3N_4, Al_2O_3, Y_2O_3, ZrO_2, TiB_2 and ZrB_2 (8, 9). In recent years, most of these reinforcements have been incorporated into $MoSi_2$ and most investigators report improvements in the toughness, strength and creep resistance over monolithic $MoSi_2$.

A critical assessment of such improvements necessarily rests on comparisons with the properties of monolithic material. Initial comparisons are usually made with a monolithic material processed in a similar fashion to the composite material. However, this may be the appropriate comparison. For example, it is well established that silica is detrimental to the properties of $MoSi_2$. If a particular composite processing route favors the incorporation of additional silica, then the resultant material may exhibit improved properties over a similarly processed monolithic material but have degraded properties compared with monolithic $MoSi_2$ processed such that it has a lower silica content. Thus, any discussion of $MoSi_2$ composites should begin with an overview of the properties of monolithic $MoSi_2$, with an emphasis on the effects of processing route on properties. This should enable us to select a set of property data that will facilitate comparisons between various composite strategies.

Monolithic Molybdenum Disilicide

Elevated Temperature Strength

Figure 1 is a plot of the yield strength as a function of temperature, obtained by either compression or bend testing, of monolithic polycrystalline $MoSi_2$. When compression testing was the method used, the initial strain rate is indicated. These materials were produced using a variety of techniques that fall into two groups. The first group involves a synthesis step from elemental powders and includes the reactive HIP of elemental powders (10), mechanical alloying of elemental powders followed by hot pressing (11,12) and hot pressing followed by HIP of reactively sintered elemental powders (13). Materials in the second group are produced by the densification of commercial $MoSi_2$ powder by either hot pressing (14, 15) or HIP'ing (16). The extreme variability in elevated temperature strength levels is a reflection of the efficacy of these various processing routes. Both the highest and the lowest strengths are exhibited by materials synthesized from elemental powders. Synthesis by mechanical alloying (MA) yields very low strength material, most likely due to the incorporation of oxygen during the milling process. MA materials have very high levels of oxygen, >1wt% (10). This translates into a very high volume fraction of SiO_2 particles with a resultant strength decrement. Reaction sintering or reaction HIP on the other hand, can lead to very low oxygen material, ≈600wppm (17). These materials retain high strength to temperatures as high as 1400°C. Materials produced from commercial powders fall between these two extremes and again the variability can be related to processing parameters. Materials densified by hot pressing (filled symbols in Figure 1) are not as strong as those produced by HIP consolidation

(empty symbols in Figure 1); this difference is probably due to the lower density of the hot pressed materials. In fact, fully dense $MoSi_2$ produced by HIP processing of commercial powder (CERAC) exhibits strengths similar to synthesized + HIPed material despite its higher oxygen content (16). Slip casting, which produces a green body from a wet powder slurry, results in lower strengths (15) compared with dry handled powder (14) when both are hot pressed. Again, this difference is probably due to impurities introduced during the processing. Figure 1 also indicates that the strength of $MoSi_2$ is strain rate sensitive, i.e. the strength increases with increasing strain rate. Strength data for NASAIR 100 (18), a "first generation" single crystal superalloy, is also plotted on Figure 1 for comparison with the $MoSi_2$ data.

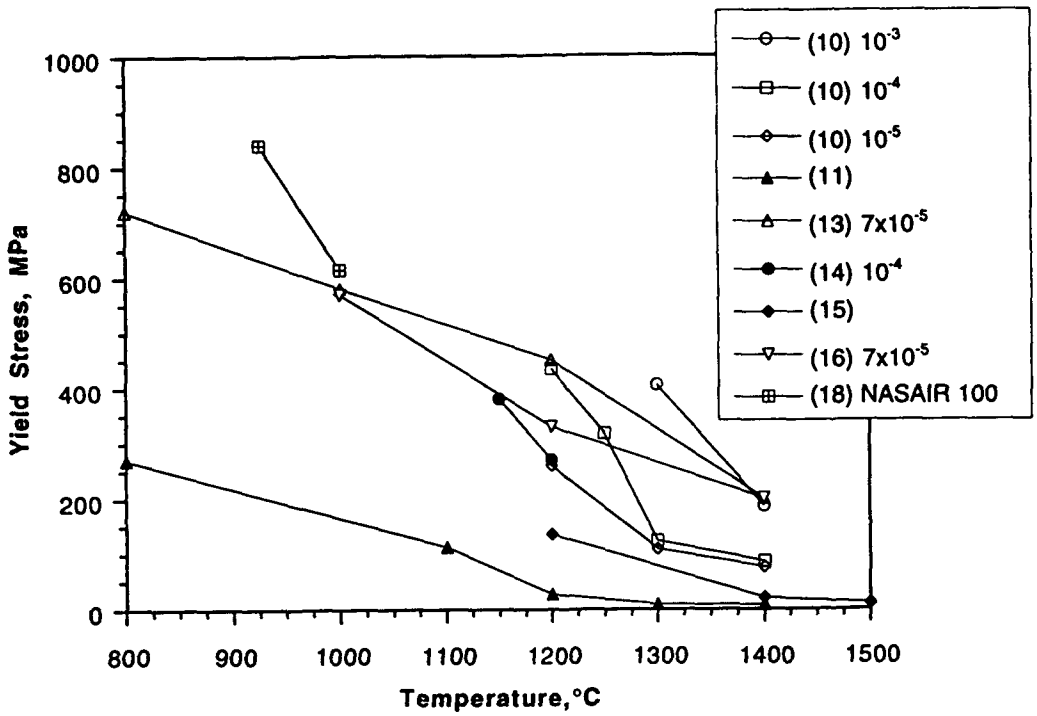

Figure 1: Yield strength of monolithic $MoSi_2$ as a function of temperature; filled symbols (●) = material consolidated by hot pressing; empty symbols (o) = material consolidated by HIP'ing.

Creep Behavior

Creep behavior is a better indicator of a material's usefulness at high temperatures than yield strength. Figure 2 shows creep data at 1200°C for monlithic $MoSi_2$ produced from commercial powder by either hot pressing or HIP'ing (19-23). Creep data at 1200°C has been plotted, as this temperature is just beyond the highest operating temperature for superalloys and therefore close to a lower operating temperature limit for advanced intermetallic-based materials. Again the material produced by HIP (empty symbols) has superior properties to that produced by hot pressing (filled symbols). Solid solution strengthening with W does not result in improved creep resistance. The superior properties exhibited by $MoSi_2$ on testing in air compared with testing in nitrogen indicate that the properties may be sensitive to testing environment (22).

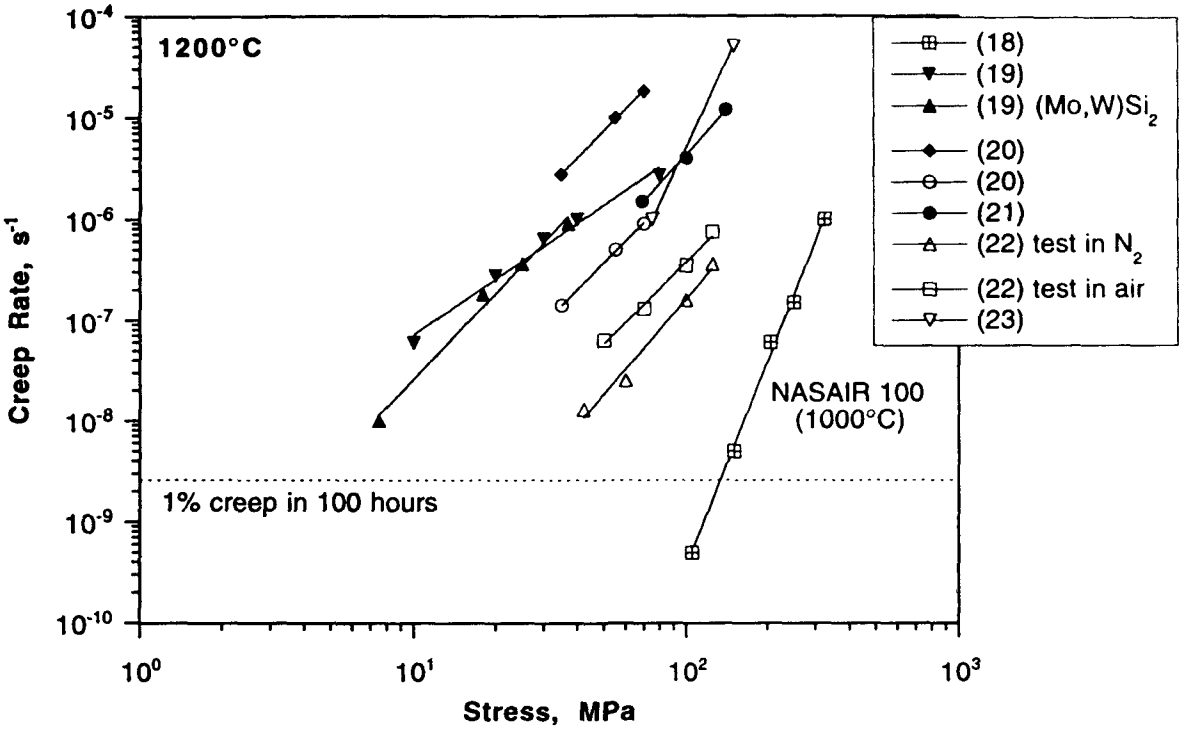

Figure 2: Compressive creep rate as a function of applied stress at 1200°C for monolithic $MoSi_2$; filled symbols (●) = hot pressed material; empty symbols (o) = HIP'ed material.

Recent work with single crystal $MoSi_2$ indicates that although it has a sufficient number of independent slip systems, the critical resolved shear stress necessary to activate the hardest orientations is extremely high at temperatures below ≈1300°C (24). A temperature of 1200°C is too low to activate the five slip systems required for the general shape change of a grain through dislocation glide. Both transgranular and intergranular microcracks have been observed in large grain (≈20-40μm) $MoSi_2$ following creep deformation at 1200°C (23). Such microcracking would be difficult to observe and, in fact, may not be present in high silica $MoSi_2$. With its very fine grain size, ≤5μm, and glassy grain boundary films, the predominant creep deformation mode in impure $MoSi_2$ is likely to be grain boundary sliding. Most researchers infer the creep deformation mechanism from the slope (n) of their creep rate versus applied stress plots coupled with a measurement of activation energy. Such indirect methods are irrelevant if the material is not deforming by mechanisms involving dislocation glide and climb processes.

The creep behavior at 1000°C of the "first generation" single crystal superalloy NASAIR 100 is also plotted on Figure 2. Typical static structures in gas turbine engines encounter stresses ≤14MPa, while rotating components such as turbine blades experience much higher stresses, ≥150MPa (20). If we ignore contributions from primary creep, we can plot a horizontal line corresponding to 1% creep in 100hrs which is a reasonable value for a structural component (25). This is the dotted line in Figure 2. The intersection of the creep curves with this line will give a value for the stress to cause 1% creep in 100 hours. Based on this data,

HIP'ed monolithic $MoSi_2$ could find application in static components at 1200°C as loads ≤16MPa will give rise to ≤1% creep in 100 hours. However, before it can be considered as a viable material for rotating components at 1200°C, $MoSi_2$ will need to be able to sustain a load of 150MPa with only ≈1% creep in 100 hours; i.e. it will need to exhibit creep properties at least comparable to those exhibited by NASAIR 100 at 1000°C.

Fracture Toughness

Unlike strength and creep resistance, fracture toughness does not appear to be highly dependent on processing variables. The ambient temperature fracture toughness of $MoSi_2$ falls in the range 3.2-5.7 MPa√m (26-31). The highest values were obtained on plasma sprayed material when the fracture toughness was measured parallel to the substrate (26, 27). These high values resulted from delamination of layers within the as-sprayed deposit (27). Diffusion bonding of the splat layers by a HIP cycle at 1200°C reduced the fracture toughness from 5.7 to 3.6 MPa√m The ductile-to-brittle transition temperature (DBTT) of HIP'ed $MoSi_2$ is ≈1300°C (10, 16). The sharpness of the brittle-to-ductile transition in $MoSi_2$ is borne out by the very modest increase, from 3.4 to 5.2 MPa√m, in the toughness of $(Mo,W)Si_2$ as the temperature is raised to 1200°C (29).

Fatigue Crack Growth

Not suprisingly, $MoSi_2$ does not exhibit stable crack growth at room temperature (32). Ramamurty et al. (29) have shown that for the monolithic material $(Mo_{0.5},W_{0.5})Si_2$, subcritical fatigue crack growth occurs over a narrow ΔK range at 1200°C; threshold occurred at $\Delta K \approx$ 3.7MPa√m and final fracture at $\Delta K \approx$ 4.2MPa√m. Detailed microstructural examination led them to state that "...controlled grain boundary cavitation and microcracking and, to a lesser extent, enhanced dislocation activity provided the mechanism for subcritical crack growth". TEM examination revealed glassy ligaments bridging the crack faces and they concluded that "cavitation induced by the viscous flow of the amorphous glass phase appears to have a decidedly more dominant effect on deformation than any dislocation plasticity..." (29).

These crack growth experiments were conducted in air. Suzuki et al. found a significant increase in the volume fraction of glassy SiO_2 phase in samples crept in air compared with samples tested in dry nitrogen (22). Diffusion of oxygen into crack tips and the highly stressed regions ahead of them will promote the formation of glassy SiO_2 and this, in concert with pre-existing glass films developed during processing from powder, will impart an apparent "ductility".

Summary

This overview of the properties of monolithic $MoSi_2$ has emphasized that increases in the strength, toughness and creep resistance will be necessary before $MoSi_2$ becomes a viable

material for hot structures, particularly hot rotating components, where the payoff will be most beneficial. Our review of the data has shown that the properties, particularly the elevated temperature strength and creep behavior, are dependent on the processing route. There are indications that the elevated temperature response of $MoSi_2$ may be sensitive to test environment; SiO_2 formation during deformation may progressively degrade properties. Finally, with this overview we have established a basis for the comparison of the properties of composite materials based on $MoSi_2$.

Composites based on $MoSi_2$

$MoSi_2$ is a line compound and has been found to be quite intolerant of alloying additions (33, 34), with the notable exception of refractory metals such as W that form isomorphous compounds with $MoSi_2$ (35, 36) and can therefore be used as solid solution alloying additions. Our review has shown however, that such additions have only a minor influence on the properties of monolithic material. Therefore, to achieve the necessary improvements in low temperature toughness coupled with increased creep resistance, researchers have focussed on a variety of composite processing approaches. The design of both ductile and brittle matrix composite materials for optimized properties continues to receive considerable attention but the basic principles are well established. Manipulation of the size, aspect ratio, volume fraction and distribution of ceramic reinforcing elements in $MoSi_2$ should lead to at least rule of mixtures strengthening and fracture toughness improvements through crack bridging and whisker or fiber pull-out. Improvements in creep properties will certainly occur if ceramic fibers are used but will probably be only minor with ceramic particulates or whiskers, unless their aspect ratio is $\geq 10:1$. The incorporation of ductile fibers or layers will obviously have a greater influence for improving toughness than ductile particulates. On the other hand, ductile particulates will probably degrade the creep resistance of $MoSi_2$. The majority of refractory metal fibers will have a similar effect as their strengths and elastic moduli are lower than that of $MoSi_2$ with W being the only exception. The incorporation of very strong W-based alloy wires, such a W-Re-HfC, may be beneficial for both toughness and creep resistance.

From this discussion it is easy to develop the impression that improving the properties of $MoSi_2$ is as simple as choosing a reinforcement and selecting a suitable processing method. However, the process is rendered more difficult by the inherent physical and chemical properties of $MoSi_2$. The chemical instability of the refractory metals in $MoSi_2$ has already been mentioned (5-7). The refractory metal silicide phases that form are brittle, so that retention of any ductilizing effect is dependent on protection of the refractory metal from interdiffusion with Si. With respect to physical properties, the high coefficient of thermal expansion (CTE) of $MoSi_2$ is a stumbling block for the production of crack-free long-fiber composites. Ideally, the thermal expansion of a fiber and matrix should be closely matched to minimize the development of stresses during processing. As illustrated in Figure 3, most of the potential refractory metal and ceramic reinforcements exhibit CTE values quite different from

$MoSi_2$. Lu et al. have shown, both theoretically and experimentally, that reducing the diameter of reinforcement fibers can lead to the elimination of brittle matrix cracking (37). An alternative approach is the addition of fine particles of a low thermal expansion phase, e.g. SiC in $MoSi_2$ (25). As shown in Figure 3, this lowers the overall CTE of the composite matrix and reduces the CTE mismatch between $MoSi_2$ and other reinforcing phases.

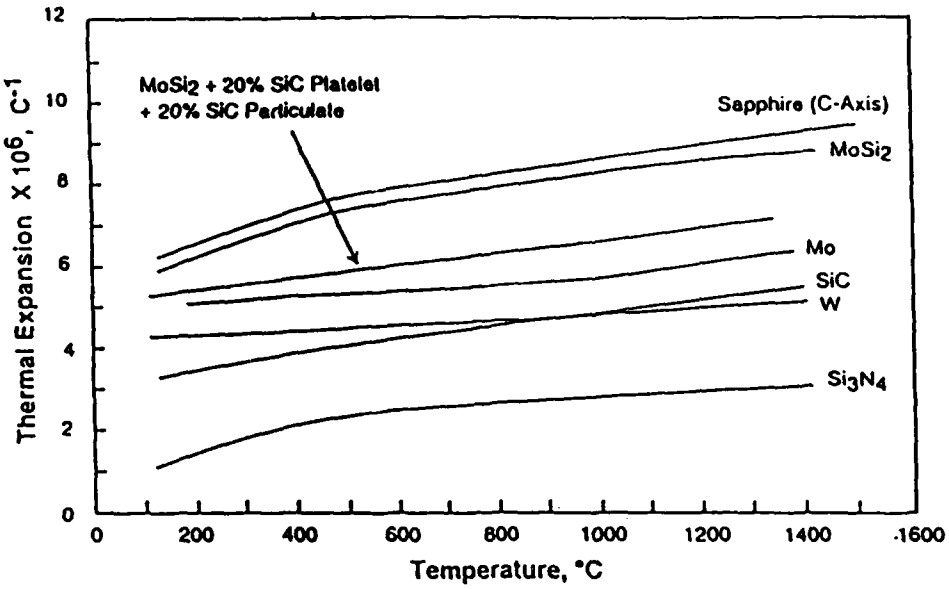

Figure 3: Mean coefficient of thermal expansion of $MoSi_2$, several potential reinforcement phases and an $MoSi_2$-SiC composite (25).

Properties of $MoSi_2$ based Composites

Having reviewed the properties of monolithic $MoSi_2$ and touched on the difficulties associated with composite processing, we will now review the progress and property improvements that have been achieved in $MoSi_2$-based composites.

Elevated Temperature Strength

Figure 4 is a plot of the compressive or flexural yield strength as a function of temperature, of a number of $MoSi_2$-based composites containing a variety of ceramic reinforcements. When an investigation included several composite variations, the data plotted is the highest reported in that investigation. Four variants of the XD™ processed composites are included as these were, by far, the strongest composites reported. The dotted line on Figure 4 is the yield strength of monolithic $MoSi_2$ processed by HIP from reactively sintered elemental powder (13, 16). The strength of the hot pressed material containing 20 vol% SiC whiskers approaches that of the HIP'ed monolithic material. The only materials that exhibit greater strength than the unreinforced material are the XD™ processed composites (13). In these materials, the yield strength was proportional to the inverse square root of the interparticle spacing, indicating that

the composite strength was due to the particle-matrix interfaces acting as obstacles to dislocation motion. A unique feature of the XD™ process is that the ceramic particles are generated in situ; they are typically high purity single crystals with clean, unoxidized interfaces. The much lower strength exhibited by the in situ composite produced by the displacement reaction between Mo_2C and Si is most probably due to the influence of impurities, particularly silica, introduced during processing (14).

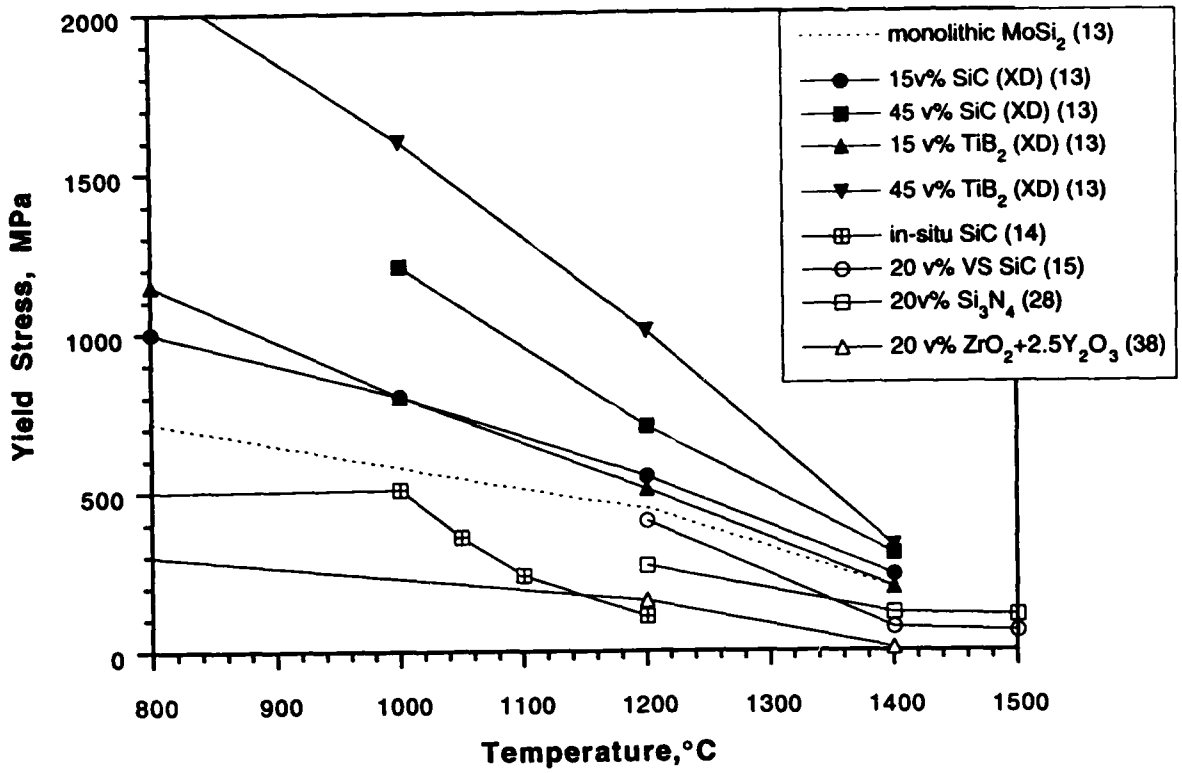

Figure 4: Yield strength of $MoSi_2$-based composites as a function of temperature; the dotted line is the yield strength of monolithic $MoSi_2$ produced by HIP of reacted elemental powders.

Creep

The steady state compressive creep rate at 1200°C of $MoSi_2$-based composites as a function of applied stress is plotted in Figure 5. The creep rate at 1200°C of HIP'ed monolithic $MoSi_2$ and the creep rate of NASAIR 100 at 1000°C are also plotted. As discussed previously, the creep rate of $MoSi_2$-based composites at 1200°C would need to approach the levels achieved by NASAIR 100 at 1000°C before it can be considered a serious contender for application in rotating aerospace components. Reinforcement with ceramic particulates can result in incremental improvements in creep strength. The true creep rate of the composite containing refractory metal particulates may be higher than the plotted values. Extensive internal oxidation of the Nb particles occurred during creep exposure and volume expansion associated with this oxidation probably neutralized a portion of the compressive creep strain leading to a lower apparent creep rate (20).

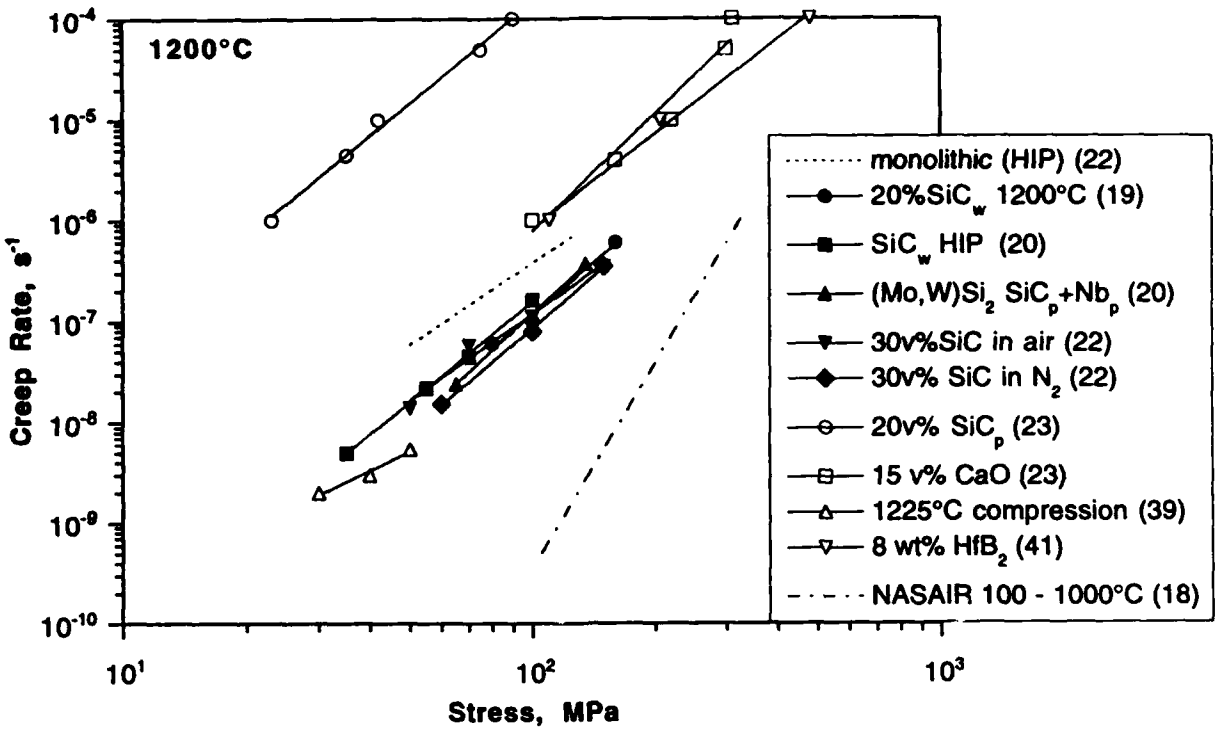

Figure 5: Compressive creep rate as a function of applied stress at 1200°C for $MoSi_2$-based composites

In the studies reported to date (20, 39), creep rates in tension are faster than those observed under compression loading. The difference in creep behavior between tension and compression is usually attributed to volume expansion due to cavity formation which contributes to the rate of creep in tension but not in compression. In both of these investigations, cavities were observed in crept tensile samples. No mention was made of cavity formation in compression samples but they have been observed by other researchers (23). Possibly, the higher creep rates observed in tension are associated with in situ silica formation as surface connnected cracks develop during deformation.

Fracture Toughness

The ambient temperature fracture toughness of $MoSi_2$-based composites containing ceramic whiskers and particulates (14, 26, 29-31, 38, 42) varies from 5.0MPa√m for hot pressed $MoSi_2$ containing 20 vol% TiC particulate (31) to 8.2MPa√m for slip cast and hot pressed $MoSi_2$ incorporating 20 vol% SiC whiskers (30). These values represent marginal increases in the fracture toughness. Some benefits of ceramic whiskers were also seen at elevated temperatures; the measured fracture toughness of both $(Mo,W)Si_2$+30vol%SiC particulate (29) and $MoSi_2$+30vol%SiC particulate produced by in situ displacement reaction (14) increased from 5-6MPa√m to 11-14MPa√m as the test temperature was increased to 1200°C. The introduction of refractory metal particulates (27, 43) also produces only

incremental improvements in fracture toughness. However, the incorporation of refractory metal layers (44, 45) and filaments (5-7, 45) can give fracture toughness values as high as 15.2MPa√m (20 vol% Nb layered and tested ⊥ to the layers).

Fatigue Crack Growth

Similar to the monolithic material, $(Mo,W)Si_2$ containing SiC particulates did not exhibit stable crack growth at room temperature (29); catastrophic fracture occurred at $\Delta K \approx$ 4.2MPa√m, a value close to the ambient temperature fracture toughness. At 1200°C, the composite exhibited a higher fatigue fracture threshold and a more extended range of stable crack growth than the monolithic material. However, Ramamurthy et al. (29) concluded that the high temperature crack growth response of the silicide matrix composite is still dominated by the pre-existing and "in-situ-formed" glass phases at intergranular and interfacial boundaries. Similar effects have also been observed in alumina and SiC-reinforced alumina composites (29).

Dève et al. (46) have investigated the ambient temperature fatigue response of $MoSi_2$-40vol% SiC matrix reinforced with 30 vol% alumina-coated Mo fibers. Their experiments were carried out on fully pre-cracked tensile specimens so that the only resistance to crack opening was provided by the fiber tractions. The results indicated that if the applied stress was below a threshold value governed by the flow stress of the ductile fibers, then the crack opening remained constant over a large number of cycles. Final failure began with the propogation of fatigue microcracking across the Mo fibers while ultimate failure involved ductile rupture of the remaining fibers.

While the data indicates that ductile phase toughnening with refractory metal fibers is an effective mechanism at ambient temperatures, the question of its efficacy under elevated temperature oxidizing conditions has not yet been addressed. Refractory metals oxidize extremely rapidly at even moderately elevated temperatures. The refractory metal fibers would need to be coated with a ceramic layer to prevent interdiffusion of silicon but it is not clear whether this layer will provide any environmental protection to exposed fibers in a cracked region.

Progess and Prospects

Despite the large amount of effort devoted to $MoSi_2$-based composites in recent years, this review demonstrates that progress has been only incremental. Marginal improvements in damage tolerance and creep resistance have been obtained by the incorporation of stable ceramic particles and whiskers. More dramatic improvements would be expected if ceramic fibers such as Saphikon or SCS6-SiC could be used but CTE mismatch problems have so far proved insurmountable; successful fabrication of an $MoSi_2$-based composite based on these

fibers has not been reported. Problems associated with fabrication of long fiber composites with refractory metal fibers are equally intractable. Some of the problems have been overcome. $MoSi_2$ composites incorporating Mo wires have been successfully fabricated using substantial volume fractions of SiC particles to reduce the CTE of the matrix and alleviate cracking during cool-down from the processing temperature. The ultimate composite using this approach would probably use fine Si_3N_4 to reduce the matix CTE and high strength W-Re-HfC wire reinforcements to impart damage tolerance and creep resistance. Stategies such as slurry and sol-gel processing have been developed for the application of diffusion barrier coatings to refractory metal fibers. However, the assurrance of coating integrity through final processing will always be a question. The development of processing techniques for the in situ coating of pre-oxidized refractory metal fibers in an $MoSi_2$ matrix containing Al (47, 48) may provide a way around this dilemma. What has developed as a result of the recent flurry of activity in this area of brittle-matrix composites is a greater understanding of not only the mechanisms of toughening and strengthening in these materials but also an appreciation for the importance of processing methods for achieving improved properties.

Acknowledgements

This work was supported by the U.S. Air Force Office of Scientific Research, Contract No. F49620-91-C-0027.

References

1. V. Bizzarri, B. Linder and N. Lindskog, Ceramic Bulletin, **68** (1989) 1834.
2. W. A. Maxwell: NACA-RM-E9G01, Lewis Flight Propulsion Laboratory (1949).
3. W. A. Maxwell: NACA-RM-E52D09, Lewis Flight Propulsion Laboratory (1952).
4. R. A. Long: NACA-RM-E50F22, Lewis Flight Propulsion Laboratory (1950).
5. E. Fitzer and F. K. Schmnidt, High Temperatures-High Pressures, **3**, 445-460 (1971).
6. J. Schlichting, High Temperatures-High Pressures, **10**, 241 (1978).
7. E. Fitzer and W. Remmele, in Proc. Fifth International Conference on Composite Materials, ICCM-V, ed. W. C. Harrigan, Jr., J. Strife and A. K. Dhingra, 515-530 (1985).
8. P. J. Meschter and S. S. Schwartz, JOM, **41**, (1989) 52.
9. A. K. Vasudevan and J. J. Petrovic, Mater. Sci. Eng., **A155**, (1992) 1.
10. D. A. Hardwick, P. L. Martin, S. N. Patankar and J. J. Lewandowski, in Proc.International Symposium on Structural Intermetallics, (1993) pp 665-674.
11. R. B. Schwarz, S. R. Srinivasan, J. J. Petrovic and C. J. Maggiore, Mat. Sci. Eng. A, **A155** (1992) 75.
12. S. R. Srinivasen, R. B. Schwartz and J. D. Embury, Mat. Res. Soc. Proc. **288**, (1993) pp 1099-1104.
13. R. M. Aiken, Mat. Sci. Eng. A, **A155** (1992) 121.
14. C. H. Henager, Jr., J. L. Brimhall and J. P. Hirth, Mat. Sci. Eng. A, **A155** (1992) 109.
15. J. J. Petrovic and R. E. Honnell, Ceramic Engineering and Science Proceedings, **11** (7-8), 734 (1990).

16. R. M. Aikin, Jr, Scripta Metall. Mater. **26**, 1025 (1992).
17. D.A. Hardwick, P.L. Martin and R.J. Moores, Scripta Metall. Mater., **27**, 391 (1992).
18. M. V. Nathal and L. J. Ebert, Metall. Trans. A, **16A** (1985) 430.
19. K. Sadananda, C. R. Feng and H. Jones, Mat. Sci. Eng. A, **A155** (1992) 227.
20. S. Bose, Mat. Sci. Eng. A, **A155** (1992) 217.
21. D. M. Shah, D. Berczik, D. L. Anton and R. Hecht, Mat. Sci. Eng. A, **A155** (1992) 45.
22. M. Suzuki, S. R. Nutt and R. M. Aiken, Jr., Mat. Res. Soc. Proc. **273**, (1992) pp 267-274.
23. A. K. Ghosh, A. Basu and H. Kung, Mat. Res. Soc. Proc. **273**, (1992) pp 259-266.
24. S. A. Maloy, T. E. Mitchell, J. J. Petrovic, A. H. Heuer and J. J. Lewandowski to be published Proc. MRS Symposium Silicides and Refractory Metals, Fall 1993.
25. M. J. Maloney and R. J. Hecht, Mat. Sci. Eng. A, **A155** (1992) 19.
26. R. Tiwari, H. Herman and S. Sampath, Mat. Res. Soc. Proc. **213**, (1991) pp 807-813.
27. R. G. Castro, R. W. Smith, A. D. Rollett and P. W. Stanek, Scripta Met. et Mater. **26** (1992) 207.
28. J. J. Petrovic and R. E. Honnell, J. Mat. Sci. Letters, **9** (1990) 1083.
29. U. Ramamurty, A. S. Kim, S. Suresh and J. J. Petrovic, J. Am. Ceram. Soc., **76** (1993) 1953.
30. D. H. Carter, J. J. Petrovic, R. E. Honnell and W. S. Gibbs, Ceram. Eng. Sci. Proc., **10**, 1121 (1989).
31. J-M. Yang, W. Kai and S. M. Jeng, Scripta Met. et Mater. **23** (1989) 1953.
32. K. T. V. Rao, W. O. Soboyejo and R. O. Ritchie, Met. Trans. A., **23A** (1992) 2249.
33. W. J. Boettinger, J. H. Perepezko and P. S. Frankwicz, Mat. Sci. Eng. A, **A155** (1992) 33.
34. P. S. Frankwicz, J. H. Perepezko and D. L. Anton, Mat. Res. Soc. Proc. **288**, (1993) pp 159-164.
35. D. M. Shah, D. Berczik, D. L. Anton and R. Hecht, Mat. Sci. Eng. A, **A155** (1992) 45.
36. A. K. Vasudevan and J. J. Petrovic, Mat. Sci. Eng. A, **A155** (1992) 1.
37. T. C. Lu, J. Yang, Z. Suo, A. G. Evans, R. Hecht and R. Mehrabian, Acta Metall. Mater. **39** (1991) 1853.
38. J. J. Petrovic, A. K. Bhattacharya, T. E. Mitchell, R. K. Wade and K. J. McClellan, Mat. Sci. Eng. A, **A155** (1992) 259.
39. S. M. Wiederhorn, R. J. Gettings, D. E. Roberts, C. Ostertag and J. J. Petrovic, Mat. Sci. Eng. A, **A155** (1992) 209.
40. H. E. Dève, C. H. Weber and M. J. Maloney, Mat. Sci. Eng. A, **A153** (1992) 668.
41. R. Ray and J. D. Whittenberger, J. Mat. Sci. Letters, **12** (1993) 260.
42. S. Maloy, J. J. Lewandowski, A. H. Heuer and J. J. Petrovic, Mater. Sci. Eng., **A155**, (1992) 159.
43. R. G. Castro, R. W. Smith, A. D. Rollett and P. W. Stanek, Mater. Sci. Eng., **A155**, (1992) 101.
44. L.Xiao and R. Abbaschian, Mat. Sci. Eng. A, **A155** (1992) 135.
45. L. Xiao, Y. S. Kim, R. Abbaschian and R. J. Hecht, Mat. Sci. Eng.A, **A144** (1991) 277.
46. H. E. Dève, S. M. Spearing and M. J. Maloney, Mat. Sci. Eng. A, **A160** (1993) 209.
47. A. Costa e Silva and M. J. Kaufman, Scripta Metall. Mater. **29** (1993) 1141.
48. A. Costa e Silva and M. J. Kaufman, to be published in Processing and Fabrication of Advanced Materials III, ed. V. A. Ravi and T. S. Srivatsan, TMS, Warrendale, PA, 1994.

Appendix III

Reaction Synthesis Of $MoSi_2$ From High Purity Elemental Powders

D.A. Hardwick, P.L. Martin and R.J. Moores
Rockwell Science Center
Thousand Oaks, CA 91360

(*Scripta Metall. et Mater.*, **27**, (1992) 391–394)

Scripta METALLURGICA et MATERIALIA
Vol. 27, pp. 391-394, 1992
Printed in the U.S.A.
Pergamon Press Ltd.
All rights reserved

REACTION SYNTHESIS OF $MoSi_2$ FROM HIGH PURITY ELEMENTAL POWDERS

D. A. Hardwick, P. L. Martin and R. J. Moores
Rockwell International Science Center
Thousand Oaks, CA 91360

(Received May 18, 1992)

Introduction

Molybdenum disilicide ($MoSi_2$) is an intermetallic compound that combines a high melting point (2293K) with excellent resistance to high temperature oxidation [1, 2]. With respect to mechanical properties, the behavior of polycrystalline $MoSi_2$ falls into one of three regimes, based on the use temperature [1]: (1) T< 925°C : strong + brittle; (2) 925 < T < 1250°C : strong + "ductile" and (3) T > 1250°C : weak + ductile.

A number of composite designs [1] address the lack of low temperature toughness and high temperature creep resistance exhibited by $MoSi_2$. Significant successes have been achieved in increasing the low temperature behavior of $MoSi_2$ through ductile phase toughening [3, 4]. Approaches to increase the elevated temperature strength have included the addition of silicon carbide whiskers [5] and a combination of SiC reinforcement and solid solution alloying with tungsten [6].

The majority of recent investigations have focused on the properties of $MoSi_2$-based materials processed from commercially available powder. Commercial $MoSi_2$ powder contains significant amounts of oxygen; for example, a chemical analysis of powder obtained from Cerac Inc. revealed an oxygen content of 0.6 wt% [7]. Consolidation of such powder resulted in a substantial volume fraction of amorphous silica in the final product [8]. $MoSi_2$ powder produced by the crushing and grinding of arc-melted elemental Mo and Si also exhibited amorphous Si-rich particles after vacuum hot-pressing at 1973K and 30MPa [8]. Grinding of the cast material to powder was done in ethanol but once this was driven off, the powder was air-handled. The high energy mechanical alloying in an argon atmosphere of elemental Mo and Si powder to produce $MoSi_2$ has also been investigated [10, 11]. Following hot pressing, the $MoSi_2$ made in this fashion still contained a substantial volume fraction of SiO_2.

The low temperature brittleness of $MoSi_2$ dictates a composite approach to material processing for the production of a useful engineering material and this route necessarily involves powder processing. Silica appears to be an unavoidable contaminant in commercially available powder and also results when processing and/or handling steps are carried out in air. This has led to the claim that a glassy silica phase is "intrinsic" in powder processed $MoSi_2$ [8]. Careful examination of the investigations presented above reveals that, during some phase of the processing cycle, air exposure of the $MoSi_2$ powder occurred. If air exposure is avoided, then production of silica-free $MoSi_2$ should be possible. The present study was undertaken to assess the feasibilty of the direct formation of $MoSi_2$ from high purity elemental powders when oxygen contamination is minimized at each step in the processing.

Experimental

High purity powders of molybdenum and silicon were obtained from commercial vendors. The highest priority was placed on obtaining powders with low oxygen contents. Both powders were packed under inert gas by the vendor. The Mo powder with a particle size of ~5μm had an analyzed oxygen content of 600 wppm oxygen. The silicon powder was larger in size at ~80μm with analyzed oxygen content of 20 wppm.

To ensure an intimate mixture of the Mo and Si, the elemental powders were ball-milled in an evacuated 300mm diameter stainless steel container using 12mm diameter tungsten carbide balls; the rotation speed was 70 rpm. A powder charge weighing ~1kg was used and each charge consisted of the correct amounts of Mo and Si powder to yield stoichiometric $MoSi_2$. The ball:powder weight ratio was 6:1 and no dispersants or additives were used in the milling operation. Powder weighing and loading into the ball mill canister were done in an argon atmosphere glove

0956-716X/92 $5.00 + .00
Copyright (c) 1992 Pergamon Press Ltd.

box (<2wppm oxygen). The canister was evacuated inside the glove box prior to transfer to the rotation device. The vacuum level in the canister was checked at the end of the 24 hour milling time as a sensitive measure of the cleanliness of the operation. Following ball milling, the canister was transferred back into the glove box and the powder mixture was removed and tightly packed into a flexible rubber sleeve which was then sealed and evacuated to a measured pressure of $4x10^{-3}$ Pa. Cold isostatic pressing (CIP) was then accomplished at 200 MPa for 30 minutes. This initial CIP step produced a "green" body with a measured density of 67%. This "green body" had sufficient strength to permit lathe turning to a tight tolerance prior to its placement within cylindrical Ta HIP cans. Initially, turning of the CIP compact was done in air but this operation too was eventually transferred to an inert atmosphere. The Ta HIP cans were evacuated at 623K to a measured pressure of $1.3x10^{-4}$ Pa prior to sealing. The HIP operation was carried out to a maximum pressure of 200 MPa and a maximum furnace temperature of 1672K. The selection of HIP temperature was based on differential thermal analysis (DTA) experiments designed to probe the parameters of the exothermic reaction between Mo and Si to produce $MoSi_2$. A DTA scan was performed on a ball milled, cold-pressed powder mixture at a heating rate of 40K/min. A series of HIP cycles were run, using the selected maximum temperature, to determine the time-temperature profile for optimum processing.

Following consolidation, the materials were characterized using X-ray diffraction and a variety of metallographic techniques. Optical microscopy of $MoSi_2$ was facilitated by its tetragonal crystal structure; the grain structure of anisotropic materials is revealed under polarized light. $MoSi_2$ and Mo_5Si_3 could be distinguished from each other optically by morphology and color but the most definitive evidence was obtained from back-scattered contrast in the scanning electron microscope coupled with energy dispersive X-ray analysis. The oxygen content of each of the materials after reaction synthesis/consolidation was determined using standard vacuum fusion techniques.

Results and Discussion

X-ray analysis of the elemental powder mixture after ball milling showed no evidence of either amorphization or compound formation. SEM examination confirmed that mechanical mixing, particle welding and comminution are the only processes taking place in the milling operation. This is shown in Figure 1 which illustrates a composite Mo+Si particle after 24 hours of ball milling. Under the compressive deformation conditions of the ball milling operations, the Mo was ductile and developed a lamellar structure. The Si remained brittle but fracturing led to refinement of the particle size. The goal of the ball milling was the production of a refined microstructure containing an intimate mixture of the original constituents. This microstructural refinement should enhance the subsequent processing steps, namely simultaneous consolidation and reaction to form monolithic $MoSi_2$.

DTA scans performed on a ball-milled and cold-pressed sample exhibited a large exotherm at 1590K during the first heating cycle. Subsequent cool down and heat up cycles showed no further deviations from linearity indicating that the initial exotherm coincided with the reaction of Mo and Si to form $MoSi_2$. The reaction onset temperature was well below both the melting temperature of silicon (1687K) and the Mo-Si eutectic temperature (1673K) indicating that the reaction initiated in the solid state. This low ignition temperature has been corroborated in a recently reported investigation of self-propagating synthesis of $MoSi_2$ [11]. In this work, an ignition temperature of 1217K was noted, although the measurement technique used was subject to numerous errors. Therefore, based on our own data and the experimental results of other investigators, a HIP temperature of 1673K was selected as more than sufficient to ensure ignition of the exothermic reaction. The heat liberated by the exothermic reaction would then raise the temperature of the material in the HIP can beyond 1673K, ensuring a dense product in conjunction with the applied 200MPa isostatic pressure. The adiabatic temperature for the reaction of $MoSi_2$ from its constituent elements at room temperature, i.e. the maximum attainable temperature dictated by the heat of formation and the specific heat of the reactants and the product, has been calculated [12] to be 1913K. This temperature will increase, as will the reaction kinetics, with increasing powder compact density and increasing pre-heat temperature. Given the high initial density of the powder compact and a pre-heat temperature equal to the ignition temperature, the maximum temperature attained by the powder due to the exothermic reaction was probably close to the melting temperature of $MoSi_2$.

The conditions chosen for the initial HIP were: 1hour to 1673K, 1hour hold, 4 hour ramp to RT. The pressure was allowed to increase with the temperature to a maximum of 200MPa. Following this HIP cycle, the powder had completely reacted to form $MoSi_2$ but the product was cracked and quite porous. This cracking and porosity could have arisen from two causes. The primary cause was most likely the relatively fast cool down rate to ambient temperature. $MoSi_2$ has a non-cubic crystal structure which results in highly directional CTE values. Thus polycrystalline $MoSi_2$ is quite prone to cracking if cooled at a rate that is too high to permit accommodation of the CTE within the microstructure. To alleviate this source of cracking, the time for cool down from 1673K to room temperature was increased from 4 to 12 hours. A further cause of the porosity and cracking was the possibility of non-uniformity of ignition of the exothermic reaction. The ramp to 1673K over 1 hour might not provide sufficient time for the entire powder compact to come to a uniform temperature. This would result in non-homogeneous

ignition of the reaction. The porosity was concentrated towards the center of the HIP can; this could arise if ignition of the reaction occurred first at the outer edge of the compact. Consequently, a short hold at 1373K was programmed into the HIP temperature profile; this hold at 1373K, well below the reaction temperature, should allow the powder compact to equilibrate to a uniform temperature prior to initiation of the exothermic reaction.

The incorporation of both of these modifications resulted in the following HIP cycle which was used for all subsequent runs: 1 hour to 1373K, 30 minute hold, 1 hour to 1673K, 1 hour hold, 12 hour ramp to RT with the pressure rising and falling with the temperature. Material reacted using this HIP cycle was dense and exhibited only minor amounts of cracking around the perimeter of the HIP can. The microstructure of this material is shown in Figure 2 and an X-ray spectrum in Figure 3. Chemical analysis revealed that this material contained 3500 wppm oxygen. $MoSi_2$ has a very low solubility for oxygen so the majority of this oxygen is present as SiO_2, seen in the microstructure in Figure 2 as small dark particles. The average grain size is 5-10μm, comparable with that observed by other investigators for consolidated commercial $MoSi_2$ powder, see for example [8]. A further consequence of the presence of SiO_2 in the structure is a measurable amount of Mo_5Si_3. Consumption of Si to form SiO_2 renders the material slightly Mo-rich leading to the formation of Mo_5Si_3. This can be seen in the X-ray spectrum shown in Figure 3; the minor peaks in the 2q range from 35° to 45° arise from this phase.

The SiO_2 in the synthesized product arose because the material for the initial HIP runs was not processed in a completely inert fashion. The machining of the powder compacts was done in air and this inevitably led to oxygen contamination of the material. Oxidation of the powders was amply demonstrated by a rise in the temperature of the CIP compact when it was removed from the inert atmosphere of the glovebox prior to machining. To eliminate this source of contamination, the turning of the CIP preforms for subsequent runs was accomplished in an inert atmosphere glove box. The results of this total inert handling were manifested in both the chemical composition and the microstructure of the resultant $MoSi_2$. Inertly processed material contained only 1600wppm oxygen compared with the 3500 wppm measured previously. As shown in Figure 4, the higher purity material has a much larger grain size than either the initial reaction HIP material or consolidated commercial $MoSi_2$. In these latter materials, SiO_2 particles hinder grain growth resulting in finer grains.

Summary

The feasibilty of using the exothermic reaction between Mo and Si for the synthesis of $MoSi_2$ has been demonstrated. High purity Mo and Si powders were used and all of the powder handling steps were done in a low oxygen, inert gas environment to explore the limits of the precautions that are necessary to eliminate SiO_2 contamination from powder processed $MoSi_2$. The inclusion of a ball-milling operation in the processing sequence to form an intimate mixture of the Mo and Si appeared to facilitate the subsequent reaction step. The exothermic reaction initiated at a temperature below the melting point of either Si or the Mo-Si eutectic. The heat generated in the exothermic reaction process appeared to aid the densification process as the resultant $MoSi_2$ was fully dense at a low HIP temperature (1673K) and with only moderate applied pressure (200MPa).

Acknowledgements

This work was supported by the U.S. Air Force Office of Scientific Research, Contract No. F49620-91-C-0027, under the direction of Dr A. H. Rosenstein. The authors also acknowledge M. A. Cunningham who performed the differential thermal analysis.

References

1. P. J. Meschter and D. S. Schwartz, JOM, 41(11), 52 (1989).
2. E. W. Lee, J. Cook, A. Khan, R. Mahapatra and J. Waldman, JOM 43(3), 54 (1991).
3. E. Fitzer and W. Remmele, Proc. 5th Int. Conf on Composite Materials, ICCM-V, ed. W. C. Harrigan, Jr, J.Strife and A. K. Dhingra, p 515, AIME, Warrendale, PA (1985).
4. T. C. Lu, A. G. Evans, R. G. Hecht and R. Mehrabian, Acta Met.et Mater. 39, 1853 (1991).
5. W. S. Gibbs, J. J. Petrovic and R. E. Honnell, Ceram. Eng. Sci. Proc. 8, (1987) 645 (1987).
6. J. J. Petrovic and R. E. Honnell, Ceram. Eng. Sci. Proc. 11, 734 (1990).
7. R. M. Aiken, Ceram. Eng. Sci. Proc. 12, 1643 (1991).
8. J. D. Cotton, Y. S. Kim and M. J. Kaufmann, Mat. Sci. Eng. A144, 287 (1991).
9. Y. S. Kim, M. R. Johnson, R. Abbaschian and M. J. Kaufman, Mat. Res. Soc. Symp. Proc. 213, 839 (1991).
10. S. Jayashankar and M. J. Kaufman, Scripta Met. et Mater. 26, 1245 (1992).
11. S. C. Deevi. J. Mat. Sci. 26, 3343 (1991).
12. S. Zhang and Z. A. Munir, J. Mat. Sci. 26 (1991) 3685.

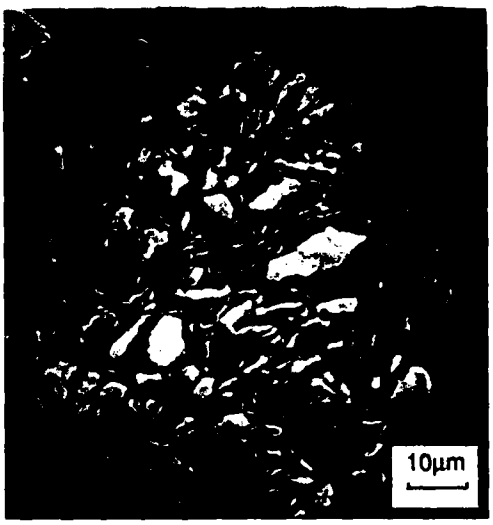

Figure 1: Back-scattered electron image of the powder mixture after 24 hours of ball milling.

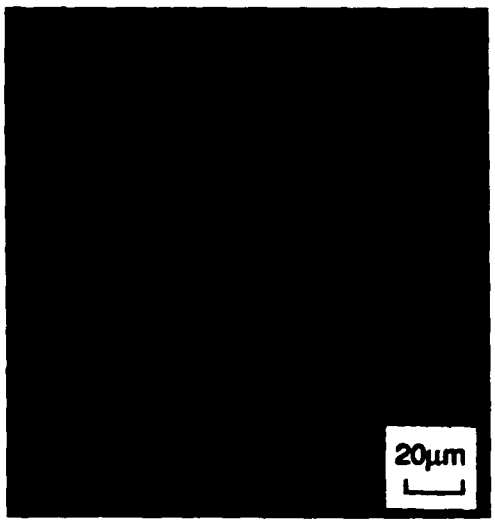

Figure 2: Microstructure of reaction HIP'ed $MoSi_2$; oxygen content was 3500 wppm.

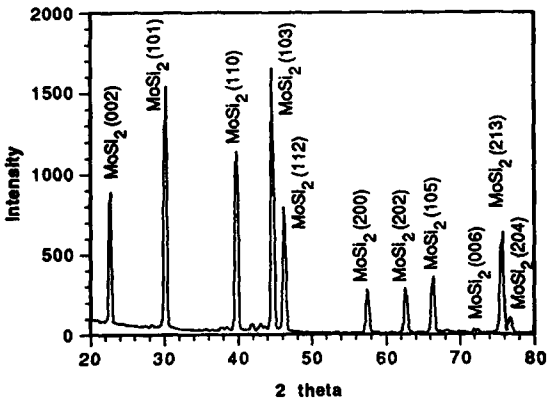

Figure 3: X-ray spectrum from HIP'ed $MoSi_2$. The minor peaks between 35° and 45° are from Mo_5Si_3.

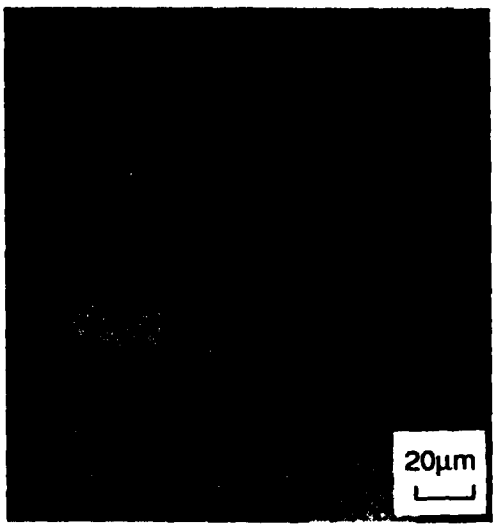

Figure 4: Microstructure of $MoSi_2$ inertly processed prior to reaction HIP. Oxygen content was 1600 wppm.

Appendix IV

Microcracking, Strain Rate and Large Strain Deformation Effects In Molybdenum Disilicide

D.A. Hardwick and P.L. Martin
Rockwell Science Center
Thousand Oaks, CA 91360

(MRS *Proceedings:* Silicides and Refractory Metals, Fall '93.)

MICROCRACKING, STRAIN RATE AND LARGE STRAIN DEFORMATION EFFECTS IN MOLYBDENUM DISILICIDE

D. A. HARDWICK AND P. L. MARTIN
Rockwell International Science Center, 1049 Camino Dos Rios, Thousand Oaks, CA 91360

ABSTRACT

High purity molybdenum disilicide was deformed in compression to strains ranging from 5 to >50%. The deformation was accomplished at temperatures in the range 1200°-1400°C and at strain rates from 10^{-3} to 10^{-5} sec^{-1}. The strength of this high purity material was found to be at least twice that of $MoSi_2$ produced by the hot pressing of commercial powder. Microstructural examination revealed that subgrain formation resulted from modest strains (≈10%) while dynamic recrystallization was observed following large strains. Transmission microscopy revealed a significant change in the dislocation substructure after straining as the temperature was increased from 1300°C to 1400°C.

INTRODUCTION

Molybdenum disilicide ($MoSi_2$) is an intermetallic compound that combines a high melting point (2293K) with excellent resistance to high temperature oxidation [1, 2]. These attributes make it a candidate structural material for use at temperatures in the 1200°-1600°C range. At ambient and moderate temperatures $MoSi_2$ is brittle, but once the ductile-to-brittle transition temperature (DBTT) is exceeded, it rapidly loses strength. The actual value of the DBTT has been a subject of some debate [3-6]. However, the oxygen content of $MoSi_2$ is often not reported but it could have a determining influence on the DBTT. The oxygen will be present as SiO_2 located at grain boundaries, triple points and within the grains [7, 8]. The behavior of the silica may dominate the material response at high temperatures, analogous to the dominant effect of sintering aids on the creep behavior in some ceramics [9]. While the presence of silica may lower the DBTT [4], this effect must be achieved at the expense of material strength. The present investigation was undertaken to provide additional information on the intrinsic deformation behavior of polycrystalline $MoSi_2$ through deformation of high purity material with a low oxygen content.

EXPERIMENTAL PROCEDURE

The $MoSi_2$ was produced by reaction synthesis during HIP processing. High purity powders of molybdenum (600 wppm oxygen) and silicon (20 wppm oxygen) in the correct weight ratio to ensure stoichiometric $MoSi_2$ were ball milled in vacuum to ensure an intimate mixture of the powders. The powder mixture was cold isostatically pressed at 200 MPa for 30 minutes, lathe turned to size and placed within cylindrical Ta HIP cans that were evacuated at 350°C prior to sealing. All of the powder handling and machining steps were done in a low oxygen, inert gas environment to limit oxygen exposure and reduce SiO_2 contamination. HIP'ing was carried out at 200 MPa and a maximum furnace temperature of 1400°C. More complete details of the processing have been published elsewhere [10]. Right circular cylinders

for compression testing were electro-discharge-machined from the HIP compacts; an average cylinder was 9.5mm in diameter by 10mm long. The ends of the cylinders were polished flat and perpendicular to the cylinder axis. Compression testing was performed over a range of strain rates from $1x10^{-3}$ to $1x10^{-5}$ sec^{-1}. All testing was conducted in a vacuum of $5x10^{-3}$ Pa or better and at temperatures in the range 1200° to 1400°C. The majority of the tests were terminated at strains of 5-6% but some were allowed to proceed to higher strains, up to ≈50% at 1300°C at 10^{-4} and 10^{-5} sec^{-1}. The compression platens were silicon nitride and the specimens were lubricated with boron nitride to reduce frictional effects. After testing, the cylinders were sectioned vertically and the microstructures examined optically and in the SEM. Specimens for TEM examination were prepared by ion milling and examined at 300keV in a Philips CM30.

RESULTS AND DISCUSSION

The reaction synthesized $MoSi_2$ after HIP processing contained <1000wppm oxygen, as determined by standard vacuum fusion techniques, and was fully dense. Figure 1 shows that the microstructure of $MoSi_2$ prior to compression testing had an average grain size of 40μm. The remnant silica particles were randomly distributed. A small volume fraction of Mo_5Si_3 was present at $MoSi_2$ grain boundaries and triple points.

The 0.2% offset yield stress as a function of temperature and strain rate is plotted in Figure 2. Lines are drawn through the data at the lower strain rates to facilitate data interpretation. Also plotted in Figure 2 is data from Petrovic et al. [11] on the strength of hot pressed commercial $MoSi_2$ powder tested in bending at a constant cross-head rate of 0.05mm/min, i.e. a strain rate of $1.2x10^{-5}$ sec^{-1}. The oxygen content of this material was not reported but if we assume that it is fully dense, then the strength decriment must be attributable to a high silica content. Viscous flow of the silica would promote grain boundary sliding as a deformation mechanism and lead to lower strengths. Our data is comparable with that obtained by Aikin on testing fully dense $MoSi_2$ containing 610 wppm oxygen [3, 12].

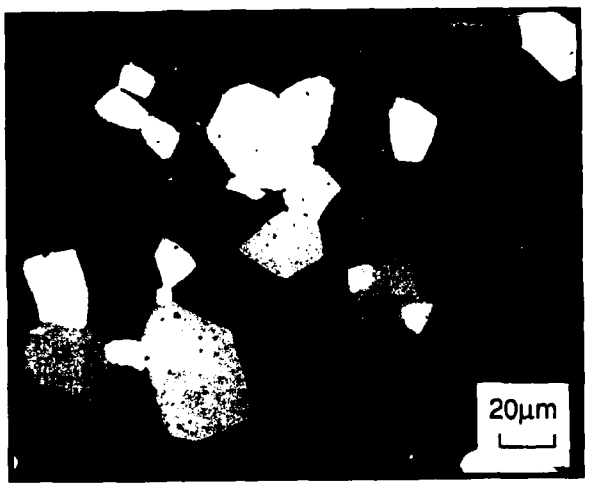

Figure 1: Microstructure of $MoSi_2$ produced by reaction HIP processing from elemental powders. Oxygen-590wppm.

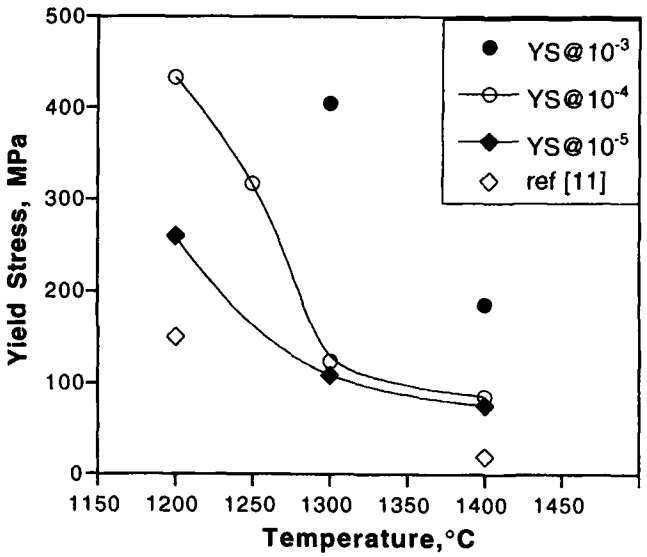

Figure 2: Compressive stress at 0.2% strain as a function of temperature and strain rate.

Metallographic examination of low strain samples, i.e. samples deformed to plastic strains ≤15%, with polarized light revealed that the grain boundaries, which were quite straight prior to deformation as shown in Figure 1, had developed a wavy character. The degree of waviness was greatest in samples that had received the highest amount of strain. Figure 3(a) shows a sample compressed 8.7% at 1250°C while the sample in Figure 3(b) was strained 15.2% at 1300°C; both were strained at a rate of 10^{-4} sec^{-1}. Both samples exhibit the wavy grain boundary effect but it is most prominent in the more highly strained sample.

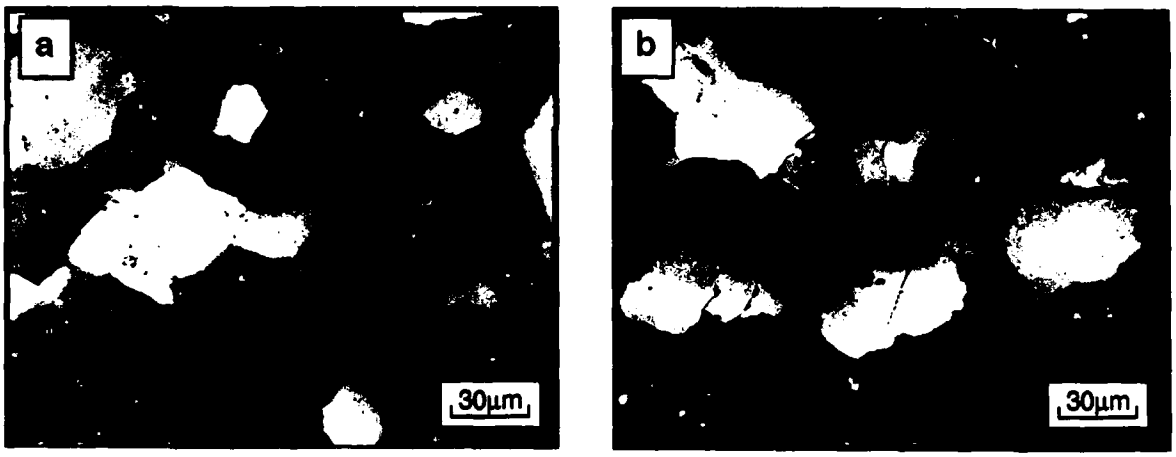

Figure 3: Microstructure in polarized light of specimens deformed (a) 8.7% at 1250°C and (b) 15.2% at 1300°C. Both specimens were compressed at an initial rate of 10^{-4} sec^{-1}.

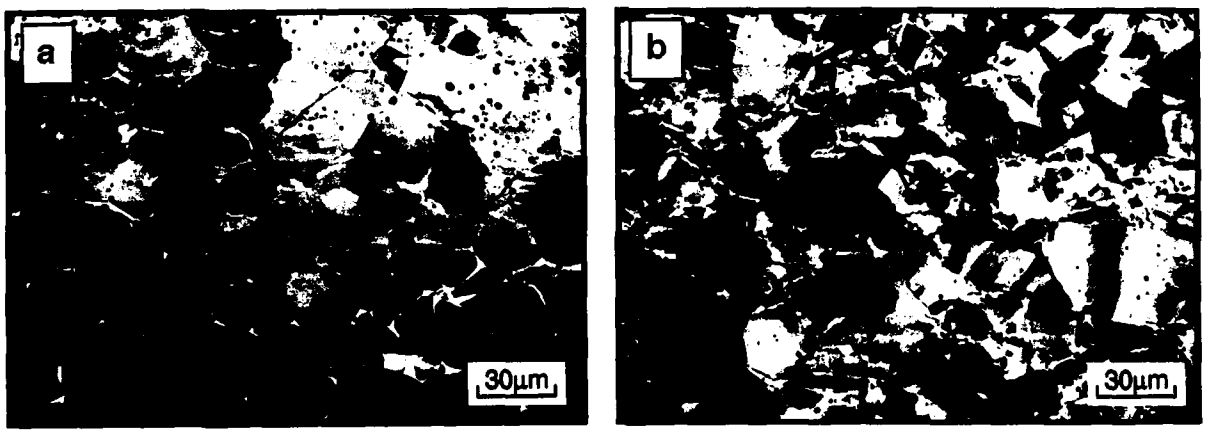

Figure 4: Microstructure revealed by backscatter SEM contrast of the samples shown in Figure 3

Examination of these same samples using backscatter contrast in the SEM reveals further differences. Backscatter imaging delineates the minor orientation differences that arise from subgrains. This contrast is well developed in the more highly strained sample of Figure 3(b) but almost absent in Figure 3(a). Examination at higher magnification showed that the waviness of the grain boundaries is associated with individual subgrains within the grains. Regardless of strain rate, deformation at 1400°C resulted in grain growth. Temperature alone was not sufficient to cause grain growth at 1400°C; a sample held at this temperature for 1 hour (a typical time to completion for a straining experiment) did not exhibit grain growth.

Figures 3 and 4 reveal another feature of these deformed samples: microcracking. None of the samples exhibited cracking on the external surfaces; this held true even for the specimens strained plastically to ≈50%. However, metallographic examination of samples sectioned longitudinally revealed that all of the samples contained internal cracks. At low strains, the interiors of the specimens contained transgranular cracks; typically, these cracks traversed just one or two grains before stopping, as shown in Figure 3. In their barreled regions, these specimens also contained intergranular cracks. Such microcracking is probably the direct result of the large variation in the critical resolved shear stress (CRSS) for glide of variously oriented $MoSi_2$ grains [13]; some orientations will be more amenable to slip than others leading to stress concentrations at grain boundaries with certain orientations. Intergranular separation could also arise from this phenomenon as adjacent grains may be unable to deform cooperatively. This effect may be exacerbated by the tensile stresses that will develop in the barreled regions of compression samples.

The microcracking was not reflected in the recorded stress-strain curves; these exhibited the usual non-linearity associated with normal plasticity and work hardening. The majority of previous investigators have not reported microcracking. In impure, high silica material, microcracking may not occur as the stress could be dissipated through viscous sliding of the grain boundary silica film before the critical stress to nucleate transgranular cracks could be achieved. The only other reported incidence of stable, transgranular microcracks was in the work of Maloy et al. [14] where transgranular micro-cracking and a non-linear load vs. displacement trace was obtained in C-containing material tested in notched bending at 1400°C.

The deformation of $MoSi_2$ to very large strains was also investigated. To avoid grain growth, samples were strained at 1300°C at strain rates of 10^{-4} and 10^{-5} sec^{-1}. The microstructure of the sample strained 48.5% at 10^{-5} sec^{-1} was quite similar to that shown in Figures 3(b) and 4(b). There was only minor distortion of the grain shape in response to the imposed strain and very limited evidence of recrystallization. On the other hand, the microstructure after 57.3% strain at 10^{-4} sec^{-1} consisted of pancake shaped grains plus significant regions of recrystallized grains. This is shown in the polarized light micrograph in Figure 5(a). The backscatter constrast micrograph in Figure 5(b) reveals the extent of subgrain formation within the deformed grains. Through dynamic recrystallization, the initially coarse microstructure has been refined significantly and it would be very interesting to know the strength of fine grained, high purity $MoSi_2$. However, the high level of strain imparted to these samples resulted in significant barreling and intergranular separation throughout much of the volume of the compression sample. The micrographs of Figure 5 were taken in the central region of the sample where grain boundary separation was minimal. The absence of significant grain refinement at the same temperature, 1300°C, but the lower strain rate of 10^{-5} sec^{-1} indicates that there is a delicate balance between the processes of grain refinement and grain coarsening at this temperature. Straining at higher temperatures would have to be done at strain

rates higher than 10^{-4} sec^{-1} to achieve similar grain refinement and grain boundary separation may remain a problem. At higher temperatures, thermally-activated modes of dislocation motion will limit stress concentrations (and therefore microcracking), but also hinder grain refinement. To achieve grain refinement, the straining must be done in a strain rate regime where such mechanisms are inoperative.

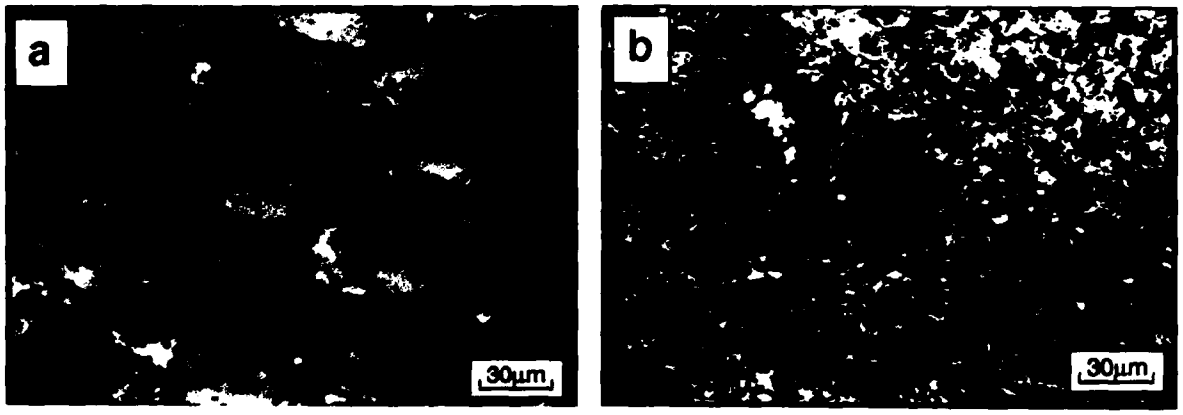

Figure 5: Microstructure of $MoSi_2$ strained to 57.3% as revealed by (a) polarized light and (b) backscatter contrast in the SEM.

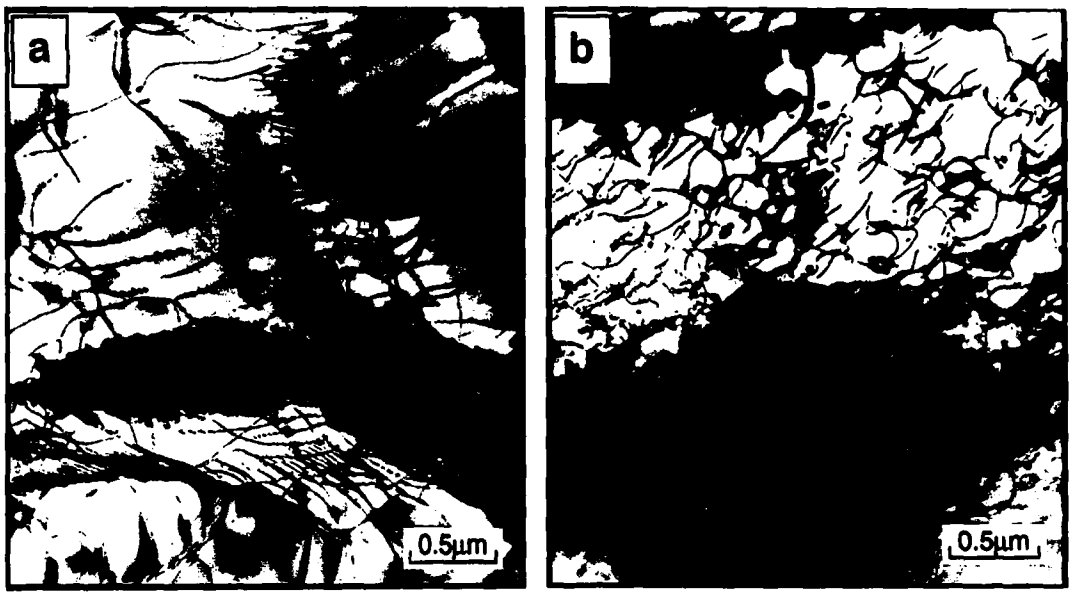

Figure 6: Dislocation substructure developed after straining at (a)1300°C and (b) 1400°C.

TEM examination revealed that straining at 1300°C and 1400°C gave rise to very different dislocation substructures; this is illustrated in Figure 6. At 1300°C, the dislocation segments are quite straight and tend to form arrays and low angle boundaries within the microstructure. At

1400°C the dislocations are quite wavy and many loops are observed. These may be indicative of thermally activated mechanisms such as dislocation climb. Work is continuing to gain a more quantitative understanding of the differences between these two dislocation substructures. However, we can conclude that there is a significant change in deformation character between 1300°C and 1400°C. This may offer definitive evidence for the intrinsic DBTT of $MoSi_2$ falling between 1300°C and 1400°C.

SUMMARY

The strength of high purity $MoSi_2$ was found to be at least twice that of hot pressed $MoSi_2$ prepared from commercial powder. After undergoing plastic strains ≤15%, subgrains developed within the original grain structure. Grain growth occurred under the combined influence of stress and temperature at the highest temperature studied, 1400°C. At higher strain levels, ≈50%, the competitive processes of dynamic recrystallization and thermally activated deformation led to grain size refinement at 1300°C after straining at 10^{-4} sec^{-1} but not at 10^{-5} sec^{-1}. The change in dislocation substructure that occurs between 1300°C and 1400°C provides corroborating evidence for the intrinsic DBTT of $MoSi_2$ occurring in this temperature range.

ACKNOWLEDGEMENTS

Supported by the U.S. Air Force Office of Scientific Research, Contract F49620-91-C-0027.

REFERENCES

1. P. J. Meschter and D. S. Schwartz, JOM, **4** (11), 52 (1989).
2. P. J. Meschter, Met. Trans A., **23A**, 1763 (1992).
3. R. M. Aikin, Jr, Scripta Metall. Mater. **26**, 1025 (1992).
4. S. R. Srinivasen, R. B. Schwartz and J. D. Embury, Mat. Res. Soc. Proc. **288**, (1993) pp 1099-1104.
5. J. Schlichting, High Temperatures-High Pressures, **10** (3), 241 (1978).
6. S. N. Patankar and J. J. Lewandowski, Mat. Res. Soc. Proc. **288**, (1993) pp 829-834.
7. J. D. Cotton, Y. S. Kim and M. J. Kaufmann, Mater. Sci. Eng., **A144**, 287 (1991).
8. S. Maloy, A. H. Heuer, J. J. Lewandowski and J. J. Petrovic, J. Am. Ceram. Soc., **74** (10), 2704 (1991).
9. D. W. Richerson, Amer. Ceram. Soc. Bull., **52** (7), 560 (1973).
10. D.A. Hardwick, P.L. Martin and R.J. Moores, Scripta Metall. Mater., **27**, 391 (1992).
11. D. H. Carter, J. J. Petrovic, R. E. Honnell and W. S. Gibbs, Ceram. Eng. Sci. Proc., **10**, 1121 (1989).
12. D. A. Hardwick, P. L. Martin, S, N, Patankar and J. J. Lewandowski, in Proc.International Symposium on Structural Intermetallics, (1993) pp 665-674.
13. T. Hirano, N. Nakamura, K. Kimura and Y. Umakoshi, Ceram. Eng. Sci. Proc. **12** (9-10) 1619 (1991).
14. S. Maloy, J. J. Lewandowski and A. H. Heuer, Mater. Sci. Eng., **A155**, 159 (1992).